

Fermi-liquid theory for the single-impurity Anderson model

Christophe Mora,¹ Cătălin Pașcu Moca,^{2,3} Jan von Delft,⁴ and Gergely Zaránd²

¹*Laboratoire Pierre Aigrain, École Normale Supérieure,
Université Paris 7 Diderot, CNRS; 24 rue Lhomond, 75005 Paris, France*

²*BME-MTA Exotic Quantum Phase Group, Institute of Physics,
Budapest University of Technology and Economics, H-1521 Budapest, Hungary*

³*Department of Physics, University of Oradea, 410087, Oradea, Romania*

⁴*Physics Department, Arnold Sommerfeld Center for Theoretical Physics and Center for NanoScience,
Ludwig-Maximilians-Universität München, 80333 München, Germany*

(Dated: June 17, 2022)

We generalize Nozières’ Fermi-liquid theory for the low-energy behavior of the Kondo model to that of the single-impurity Anderson model. In addition to the electrons’ phase shift at the Fermi energy, the low-energy Fermi-liquid theory is characterized by four Fermi-liquid parameters, which we express in terms of zero-temperature physical observables, namely the local charge and spin susceptibilities and their derivatives w.r.t. the local level position. We determine these in terms of the bare parameters of the Anderson model using Bethe Ansatz and Numerical Renormalization Group (NRG) calculations. Our low-energy Fermi-liquid theory applies throughout the crossover from the strong-coupling Kondo regime via the mixed-valence regime to the empty-orbital regime. From the Fermi-liquid theory, we determine the conductance through a quantum dot symmetrically coupled to two leads in the regime of small magnetic field, low temperature and small bias voltage, and compute the coefficients of the $\sim B^2$, $\sim T^2$, and $\sim V^2$ terms. The coefficients of T^2 and V^2 are found to change sign during the Kondo to empty-orbital crossover, while that of $\sim B^2$ remains positive. The crossover becomes universal in the limit that the local interaction is much larger than the level width.

PACS numbers: 71.10.Ay, 73.63.Kv, 72.15.Qm

I. INTRODUCTION AND SUMMARY

A. Introduction

The single-impurity Anderson model, originally introduced to describe d-level impurities such as Fe or Mn in metallic alloys [1–3], has emerged more recently as a standard tool to describe electron transport in quantum dot nanodevices [4, 5]. It covers a rich variety of behaviors and non-perturbative effects such as Coulomb blockade, spin formation, mixed-valence physics, or Kondo screening, and may well be one of the most intensely studied models in condensed matter physics. Indeed, the various extensions of the Anderson model bear relevance far beyond the scope of nanophysics and impurity physics, and constitute the fundaments of our understanding of correlated metals and superconductors, Mott insulators [6], non-Fermi-liquid systems [7], and heavy fermion materials [8].

In its simplest form, the Anderson model consists of a single spinful interacting level of energy ε_d and occupation $\hat{n}_d = \hat{n}_{d\uparrow} + \hat{n}_{d\downarrow}$, described by the simple Hamiltonian

$$H_d = \varepsilon_d \hat{n}_d + \frac{U}{2} \hat{n}_d^2, \quad (1)$$

which is coupled by a tunneling rate 2Δ to the Fermi sea of spinful conduction electrons. In the presence of a local magnetic field, the level is Zeeman-split by an additional term $(\hat{n}_{d\uparrow} - \hat{n}_{d\downarrow})B/2$ (we use units where the Lande factor times Bohr magneton give $g\mu_B = 1$). In

the non-equilibrium context of nano-devices, – also discussed here, – the level may be coupled to several leads characterized by different tunneling rates and Fermi energies, as sketched in Fig. 1. As mentioned before, this simple model exhibits a surprisingly rich behavior. In particular, in the limit of small Δ and a single electron on the level, i.e. an average charge $n_d = \langle \hat{n}_d \rangle \approx 1$, a local magnetic moment is formed on the level. In this “Kondo limit”, formally achieved for [9]

$$\varepsilon_d = -U/2, \quad U/\Delta \rightarrow \infty, \quad (2)$$

the Anderson model maps onto the Kondo model at small energies [10] and accounts for the Kondo effect [3, 11], i.e. the dynamical screening of the spin of this localized electron at low temperatures.

Despite being the realm of strong correlations, the low-energy structure of the screened Kondo state can be captured by simple means. Following Wilson’s solution of the Kondo model by the numerical renormalization group [12], Nozières realized that the low temperature behavior of the Kondo model can be described as a *local Fermi liquid*, and can be understood in terms of weakly interacting *quasiparticles*. He formulated an effective Fermi-liquid theory for these, in terms of the phase shift that a quasiparticle incurs when scattering off the screened singlet [13]. This phase shift, say $\delta_\sigma(\varepsilon, n_{\sigma'})$, depends not only on the kinetic energy ε and spin σ of the quasiparticle, but also on the entire distribution function $n_{\sigma'}(\varepsilon')$ of the quasiparticles with which it interacts. Nozières expanded this phase shift to leading order in ε and the deviation $\delta n_{\sigma'}(\varepsilon')$ of the quasiparticle distribu-

tion function from its ground-state form, and viewed the two expansion coefficients as phenomenological parameters, α_1 and ϕ_1 , called Fermi-liquid parameters. These parameters can be viewed as coupling constants in an effective Fermi-liquid Hamiltonian, which, when treated in the Hartree approximation, generates the phase shifts. The parameters α_1 and ϕ_1 can be expressed in terms of zero-temperature physical observables by exploiting the fact that the phase shifts determine, via the Friedel sum rule, the local charge and magnetization at zero temperature. In this way, both α_1 and ϕ_1 are found to be proportional to the zero-temperature impurity spin susceptibility, χ_s , whose inverse defines the Kondo temperature, T_K , the characteristic low-energy scale of the Kondo model.

Using the resulting quasiparticle Fermi-liquid (quasiparticle FL) theory, Nozières [13] was able to reconstruct all essential low temperature characteristics of the Kondo model, such as the value of the anomalous Wilson ratio (the dimensionless ratio of the impurity's contribution to the susceptibility and to the linear specific heat coefficient), $R = 2$ [12], or the quadratic temperature and magnetic field dependence of the resistivity.

Independently, Yamada and Yoshida developed a diagrammatic Fermi-liquid theory [14]: they reproduced the above-mentioned features within the Anderson model by means of a perturbative approach and demonstrated by using Ward identities that they hold up to infinite order in U .

Both the quasiparticle and the diagrammatic Fermi-liquid approaches proved to be extremely useful. The diagrammatic FL approach has been extended to orbitally degenerate versions of the Anderson model [15–18] and to out of equilibrium [19], and lead to the construction of the renormalized perturbation theory [3, 20, 21] (see also Ref. [22]) and its application to various extensions of the Anderson model [23–25]. Nozières' quasiparticle FL approach has been widely used to study non-equilibrium

transport in correlated nano-structures described by the Kondo model or generalizations thereof [26–33]. In particular, the effective Fermi-liquid Hamiltonian of the Kondo model was used to calculate the leading dependence of the conductance on temperature, bias voltage and magnetic field, and to determine the coefficients of the leading T^2/T_K , V^2/T_K^2 and B^2/T_K^2 terms, say c_T , c_V and c_B . These Fermi-liquid transport coefficients turn out to be universal numbers, because for the Kondo model the zero-energy phase shift, δ_0 , has a universal value, $\delta_0 = \pi/2$.

Surprisingly, Nozières' quasiparticle Fermi-liquid theory has not yet been extended to the case of the Anderson model (except for the special case of electron-hole symmetry [34]), although this model has a Fermi-liquid ground state in all parameter regimes [35, 36]. The reason has probably been that such a theory requires additional Fermi-liquid parameters, and no strategy was known to relate these to physical observables. In this work, we fill this gap and develop a comprehensive Fermi-liquid approach to the Anderson model, applicable also away from particle-hole symmetry [37, 38]. Our strategy is a natural generalization of that used by Nozières for the Kondo model. We develop an effective quasiparticle theory characterized by four Fermi liquid parameters (α_1 , α_2 , ϕ_1 and ϕ_2), and use these to expand the phase shifts of the quasiparticles systematically as a function of the quasiparticles' energy and distribution. Using the Friedel sum rule, we express these Fermi-liquid parameters in terms of four zero-temperature physical parameters, namely the local charge and spin susceptibilities, χ_c and χ_s , and their derivatives χ'_c and χ'_s w.r.t. the local level position ε_d . We then use the resulting Fermi-liquid Hamiltonian for the Anderson model to calculate the conductance to quadratic order in temperature, bias voltage and magnetic field, in a similar manner as for the Fermi-liquid Hamiltonian for the Kondo model. However, the Fermi-liquid transport coefficients c_T , c_V and c_B are no longer universal, but depend on χ_c , χ_s , χ'_c , χ'_s and the zero-energy phase shift δ_0 , all of which are functions of ε_d . We calculate these functions explicitly by using Bethe Ansatz and Wilson's Numerical Renormalization Group (NRG) method. We thus obtain explicit results for the ε_d dependence of c_T , c_V and c_B throughout the entire crossover from the strong-coupling Kondo regime ($-U + \Delta \lesssim \varepsilon_d \lesssim -\Delta$) via the mixed-valence regime ($-\Delta \lesssim \varepsilon_d \lesssim \Delta$) to the empty-orbital regime ($\varepsilon_d \gtrsim \Delta$).

B. Summary and overview of main results

In this subsection, we gather the main ideas of our approach and its main results in the form of an executive summary. Details of their derivation are presented in subsequent sections.

We shall focus on the quantum dot configuration in Fig. 1. In this case, the level on the dot couples only to

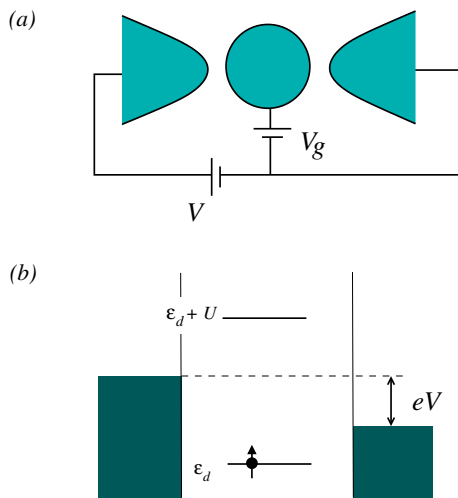


FIG. 1. Schematic picture of a quantum dot nano-device.

the ‘symmetrical’ combination of electronic states. Correspondingly, the Fermi-liquid theory can be constructed in terms of quasiparticles in ‘even’ and ‘odd’ channels, b and a , respectively [32]. Since the ‘odd’ quasiparticles do not hybridize with the d -level, the effective low-energy Fermi-liquid Hamiltonian can be constructed solely from the ‘even’ quasiparticles, and is given to leading and sub-leading order by

$$H_{\text{FL}} = \sum_{\sigma} \int_{\varepsilon} (\varepsilon - \sigma B/2) b_{\varepsilon\sigma}^{\dagger} b_{\varepsilon\sigma} + H_{\alpha} + H_{\phi} + \dots \quad (3)$$

$$H_{\alpha} = - \sum_{\sigma} \int_{\varepsilon_1, \varepsilon_2} \left[\frac{\alpha_1}{2\pi} (\varepsilon_1 + \varepsilon_2) + \frac{\alpha_2}{4\pi} (\varepsilon_1 + \varepsilon_2)^2 \right] b_{\varepsilon_1\sigma}^{\dagger} b_{\varepsilon_2\sigma}$$

$$H_{\phi} = \int_{\varepsilon_1, \dots, \varepsilon_4} \left[\frac{\phi_1}{\pi} + \frac{\phi_2}{4\pi} \left(\sum_{i=1}^4 \varepsilon_i \right) \right] : b_{\varepsilon_1\uparrow}^{\dagger} b_{\varepsilon_2\uparrow} b_{\varepsilon_3\downarrow}^{\dagger} b_{\varepsilon_4\downarrow} :,$$

where B is the magnetic field. Here α_1 , ϕ_1 , α_2 and ϕ_2 are four Fermi-liquid parameters, that can be expressed in terms of zero-temperature physical observables, as discussed below. The operators $b_{\varepsilon\sigma}^{\dagger}$ here create incoming single-particle scattering states of kinetic energy ε and spin σ , and incorporate already the zero-temperature phase shift δ_0 experienced by electrons at the Fermi energy, $\varepsilon = 0$. The term H_{α} in this expansion accounts for energy dependent elastic scattering, while the terms in H_{ϕ} describe local interactions between the quasiparticles. In the Kondo model, charge fluctuations are suppressed, and the low-energy theory exhibits electron-hole symmetry under the transformation $b_{\varepsilon\sigma}^{\dagger} \leftrightarrow b_{-\varepsilon\sigma}$. In the presence of such symmetry, the parameters α_2 and ϕ_2 must vanish, since their presence would violate electron-hole symmetry. Furthermore, as shown by Nozières [13], the parameters α_1 and ϕ_1 are equal in the Kondo model. Therefore the Kondo model’s effective FL theory (3) is characterized by a single Fermi-liquid scale, E^* , defined as

$$E^* \equiv \frac{\pi}{4\alpha_1}, \quad (4)$$

and identified as the Kondo temperature, $E^* = T_K$. In contrast, in the generic Anderson model, three of the four Fermi-liquid parameters are independent (more precisely, each of them is a function of three variables, Δ , and the dimensionless ratios ε_d/U and ε_d/Δ), and therefore the low-energy behavior cannot be characterized by a single Fermi-liquid scale. Nevertheless, we shall still use Eq. (4) to define the characteristic energy scale E^* and express physical quantities in terms of it. We emphasize that whereas the calculation of Nozières accounted only for local spin excitations, our approach includes both spin and charge fluctuations and allows us to capture the mixed-valence regime and smoothly interpolate between the Kondo and Coulomb blockade regions.

To make use of the Fermi-liquid theory in its full power, we shall determine the Fermi-liquid parameters in Eq. (3) in terms of the bare parameters of the Anderson model, U , ε_d , and Δ . To this end, we shall first demonstrate

that the four FL parameters of the Anderson model are directly related to zero-temperature physical observables, and can be expressed solely in terms of the local charge (χ_c) and spin (χ_s) susceptibilities of the Anderson model and their derivatives (χ'_c and χ'_s) with respect to ε_d ,

$$\frac{\alpha_1}{\pi} = \chi_s + \frac{\chi_c}{4}, \quad \frac{\alpha_2}{\pi} = -\frac{3}{4}\chi'_s - \frac{\chi'_c}{16}, \quad (5a)$$

$$\frac{\phi_1}{\pi} = \chi_s - \frac{\chi_c}{4}, \quad \frac{\phi_2}{\pi} = -\chi'_s + \frac{\chi'_c}{4}. \quad (5b)$$

We then determine the FL parameters from these relations, by computing the susceptibilities $\chi_c(\varepsilon_d, \Delta, U)$ and $\chi_s(\varepsilon_d, \Delta, U)$ from Wilson’s Numerical Renormalization Group method [12, 36] (NRG) and, complementarily, by computing the Bethe Ansatz solution to the Anderson model [39, 40].

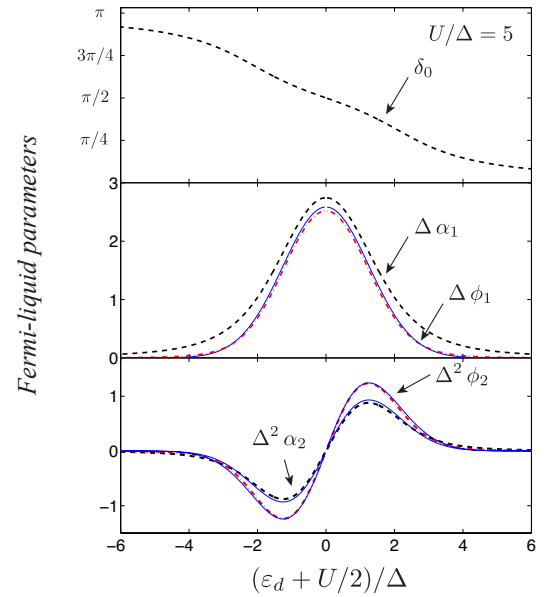


FIG. 2. (Color online) Fermi-liquid parameters, $\alpha_{1,2}$ (dashed line) and $\phi_{1,2}$ (dash-dotted line), in units of $1/\Delta$ (or $1/\Delta^2$), as functions of $(\varepsilon_d + U/2)/\Delta$ for $U = 5\Delta$, calculated from Eqs. (5), with the susceptibilities occurring therein extracted from the Bethe Ansatz computations. Charge degeneracy occurs for $\varepsilon_d + U/2 \simeq 2.5\Delta$. The thin continuous lines were computed using the analytical formulas, Eqs. (27) and (28), valid in the Kondo regime. We also include the zero-energy phase shift δ_0 (dashed line) in the top panel, obtained from the Friedel sum rule Eq. (21) (at $B = 0$) and the Bethe Ansatz calculation of n_d .

Typical results of our computations are shown in Fig. 2, where we display the four Fermi-liquid parameters for moderately strong interactions, $U/\Delta = 5$, as a function of the level’s position. In agreement with the discussion above, the parameters α_2 and ϕ_2 vanish at the electron-hole symmetrical point, $\varepsilon_d = -U/2$, and are antisymmetrical with respect to it, while the Fermi-liquid parameters α_1 and ϕ_1 display a symmetrical behavior.

In the local-moment regime, $\langle n_d \rangle \approx 1$, charge fluctuations are suppressed, and the charge susceptibility χ_c can be neglected in the expression of the Fermi-liquid parameters. Here we can derive an analytical approximation for them [Eqs. (27) and (28)] by making use of the Bethe Ansatz expression for the spin susceptibility in the local-moment regime, $\chi_s \sim T_K^{-1}$. Although Eqs. (27) and (28) are expected to be valid only for $U \gg \Delta$, even for the moderate interaction of Fig. 2, surprisingly good agreement with the complete solution is found for $|\varepsilon_d + U/2| \lesssim U/2$. In the opposite limit of an almost empty orbital, $\langle n_d \rangle \approx 0$, interactions are negligible, and transport is well described by a non-interacting resonant level model. The crossover from the local-moment to the empty-orbital regime becomes universal for large values of U , for which the dimensionless Fermi-liquid parameters, Δ/α_1 , Δ/ϕ_1 , Δ^2/α_2 , and Δ^2/ϕ_2 can be expressed as universal functions of ε_d/Δ .

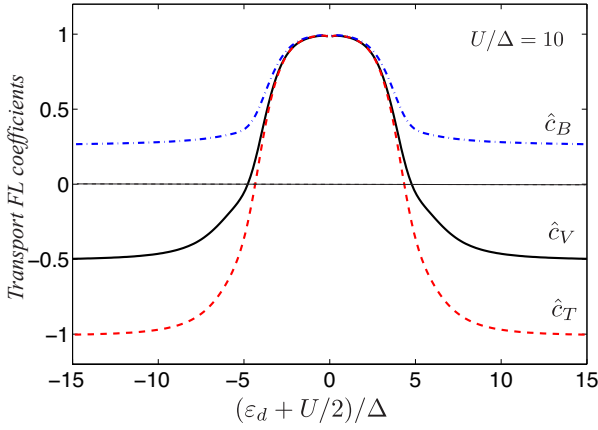


FIG. 3. (Color online) Normalized Fermi-liquid transport coefficients $\hat{c}_B \equiv c_B/c_B^K$, $\hat{c}_T \equiv c_T/c_T^K$, and $\hat{c}_V \equiv c_V/c_V^K$ as a function of the level's position, ε_d , calculated from Eqs. (7), (47) and (48). The coefficients c_T and c_V change sign as one crosses the mixed valence regime, and their ratio changes by a factor of 2, while c_B does not change sign, but its absolute value is reduced by a factor 1/2 as compared to c_V (1/4 compared to c_T). The linear conductance G_0 is shown for comparison in the top panel, in units of $2e^2/h$.

Equipped with our Fermi-liquid theory and with the four Fermi-liquid parameters, we then study a quantum dot device, coupled symmetrically to two leads, and derive exact results for the FL transport coefficients, c_V , c_T , and c_B , characterizing the conductance at low bias voltage, temperature and magnetic field,

$$G(V, T, B) - G_0 \approx -\frac{2e^2/h}{(E^*)^2} (c_T T^2 + c_V (eV)^2 + c_B B^2), \quad (6)$$

with $G_0 = (2e^2/h) \sin^2(\delta_0)$ denoting the linear conductance of the quantum dot at zero temperature and zero magnetic field. In terms of the Fermi-liquid parameters,

the coefficient c_B can be expressed, e.g., as

$$c_B = \frac{\pi^2}{64} \frac{(\alpha_2 + \phi_2/4) \sin 2\delta_0 - (\alpha_1^2 + \phi_1^2) \cos 2\delta_0}{\alpha_1^2}. \quad (7)$$

The other two coefficients c_V and c_T are expressed by similarly complex expressions, given by Eqs. (47) and (48) in Section IV B. The value of these coefficients can be trivially determined in the empty-orbital regime, where the following asymptotic values are obtained,

$$c_T^{\text{eo}} = -\frac{\pi^4}{16}, \quad c_V^{\text{eo}} = -\frac{3\pi^2}{64}, \quad \text{and} \quad c_B^{\text{eo}} = \frac{\pi^2}{64}. \quad (8)$$

Moving to the Kondo regime, the coefficients c_T and c_V change sign and their ratio changes by a factor of 2 as compared to the empty-orbital regime,

$$c_T^K = \frac{\pi^4}{16} \simeq 6.009, \quad c_V^K = \frac{3\pi^2}{32} \simeq 0.925, \quad (9)$$

reflecting the emergence of strong correlations in the Kondo regime. In hindsight, this sign change may be not very surprising: in the Kondo regime, the perfect conductance through the Kondo resonance is reduced by a finite temperature (bias), destroying Kondo coherence, while in the empty-orbital regime a gradual lifting of the Coulomb blockade is expected as the temperature or bias voltage is increased.

In contrast to c_T and c_V , the coefficient c_B does not change sign, though its absolute value increases by a factor of 2 as compared to c_V (factor of 4 compared to c_T) as one approaches the Kondo regime, where

$$c_B^K = \frac{\pi^2}{16} \simeq 0.617. \quad (10)$$

The evolution of the normalized coefficients c_V/c_V^K , c_B/c_B^K , and c_T/c_T^K is shown in Fig. 3 for $U/\Delta = 10$ as a function of the level's position, ε_d . Importantly, all three transport coefficients can be, in principle, extracted from transport measurements, and thus the predictions of this Fermi-liquid theory can be verified by straightforward transport measurements [41].

The rest of this paper is organized as follows. In Sec. II, we construct the basic Fermi-liquid theory for the Anderson model and relate the Fermi-liquid parameters of the effective Hamiltonian H_{FL} to physical observables [(5)]. In Sec. III we construct the current operator and set the framework for non-equilibrium calculations, which we then use to compute the expectation value of the current perturbatively. The final form of the transport coefficients is presented in Sec. IV, while Sec. V is devoted to a detailed discussion of our results and the conclusions. For completeness, we also included Appendix A, where we summarize the Bethe Ansatz equations and some of the integral formulas derived from them, which we used to determine the susceptibilities. Details of the perturbative calculations in the empty orbital regime are given in Appendix B.

II. FERMI-LIQUID THEORY

In this section, we present our Fermi-liquid theory for the Anderson model. The Fermi-liquid theory is by essence a perturbative approach. It gives the expansion of observables at bias voltages and temperatures smaller than the Kondo temperature T_K . We begin in Sec. II A by a reminder of the Fermi-liquid approach to the Kondo model, as introduced by Nozières [13, 42], and explain in detail how the model's invariance, in the wide-band limit, under a global energy shift can be used to relate the different Fermi-liquid parameters. In Sec. II B, we extend this approach to the Anderson model. In Sec. II C, we take advantage of the Friedel sum rule to express all Fermi-liquid parameters in terms of the spin and charge susceptibilities, see Eqs. (5), a result of considerable practical importance. The spin and charge susceptibilities are simple ground state observables – and can be computed semi-analytically by Bethe Ansatz – while the Fermi-liquid theory is able to deal with more complicated situations, such as finite temperature or out-of-equilibrium settings. Analytical expressions of the Fermi-liquid parameters are obtained in the Kondo and empty-orbital limits in Sec. II D. Finally, the effective Fermi-liquid Hamiltonian, applicable at low energy and already advertised in Eq. (3), is discussed in Sec. II E.

A. Kondo model

We begin by briefly reviewing Nozières' local Fermi-liquid theory for the Kondo model. The main ideas are well established – for details we refer to the seminal papers of Nozières [13] or to Refs. [20, 26, 31]. Our goal here is to phrase the arguments in such a way that they will generalize naturally to the case of the Anderson model, discussed in the next subsection.

For energies well below the Kondo temperature, the reduction of phase-space for inelastic processes implies that elastic scattering dominates, due to the same phase-space argument [43, 44] as in conventional bulk Fermi liquids. The system can then be characterized by the phase shift, $\delta_\sigma(\varepsilon, n_{\sigma'})$, acquired by a quasiparticle with kinetic energy ε and spin σ that scatters off the screened Kondo singlet (the form of this phase shift can be derived explicitly from the effective Fermi-liquid Hamiltonian Eq. (3) [with $\alpha_2 = \phi_2 = 0$], as explained in Sec. II E below). Since the singlet has a many-body origin, $\delta_\sigma(\varepsilon, n_{\sigma'})$ depends not only on ε but also on the quasiparticle distribution functions $n_\uparrow(\varepsilon')$ and $n_\downarrow(\varepsilon')$. Our goal is to find a simple description of this phase shift function, valid for small excitation energies relative to the ground state.

In equilibrium and at zero temperature and magnetic field, the quasi-particle ground state is characterized by a well-defined zero-temperature chemical potential μ_0 . Let ε_0 be an arbitrary reference energy, different from μ_0 , which serves as the chemical potential of a reference ground state with distribution function $n_{\varepsilon_0}^0(\varepsilon) =$

$\theta(\varepsilon_0 - \varepsilon)$. We then Taylor-expand the phase shift around this reference state as

$$\delta_\sigma(\varepsilon, n_{\sigma'}) = \delta_0 + \alpha_1(\varepsilon - \varepsilon_0) - \phi_1 \int_{\varepsilon'} \delta n_{\bar{\sigma}, \varepsilon_0}(\varepsilon'), \quad (11)$$

with $\delta n_{\sigma', \varepsilon_0} = n_{\sigma'} - n_{\varepsilon_0}^0$. The last term accounts for local interactions with other quasiparticles, and $\bar{\sigma}$ denotes the spin opposite to σ , since by the Pauli principle local interactions can involve only quasiparticles of opposite spins. We should stress that the distributions $n_{\sigma'}(\varepsilon')$ can be anything (finite temperature, voltage, magnetic field or even out-of-equilibrium distributions), as long as the expansion variables $\varepsilon - \varepsilon_0$ and $\int_{\varepsilon'} \delta n_{\bar{\sigma}, \varepsilon_0}(\varepsilon')$ in Eq. (11) are small compared to the Fermi-liquid scale E^* [45]. The Taylor coefficients δ_0 , α_1 and ϕ_1 serve as the Fermi-liquid parameters of the theory. Their dependence on ε_0 drops out in the wide-band limit considered here, and they are universal coefficients.

Now, the key point is to realize that the function $\delta_\sigma(\varepsilon, n_{\sigma'})$ is of course independent of the reference energy ε_0 used for its Taylor expansion. Differentiating Eq. (11) w.r.t. ε_0 (and noting that $\delta n_{\bar{\sigma}, \varepsilon_0}(\varepsilon')$ depends also on ε_0) one thus obtains $d\delta_\sigma(\varepsilon, n_{\sigma'})/d\varepsilon_0 = \phi_1 - \alpha_1 = 0$, or

$$\alpha_1 = \phi_1. \quad (12)$$

This relation constitutes one of Nozières' central Fermi liquid identities for the Kondo model.

As can be checked easily, Eq. (12) guarantees that for any distribution $n_{\sigma'}$ with a well-defined chemical potential, e.g. $n_\mu(\varepsilon') = (e^{(\varepsilon' - \mu)/T} + 1)^{-1}$ for nonzero temperature, the phase shift $\delta_\sigma(\varepsilon, n_\mu)$, depends on energy and

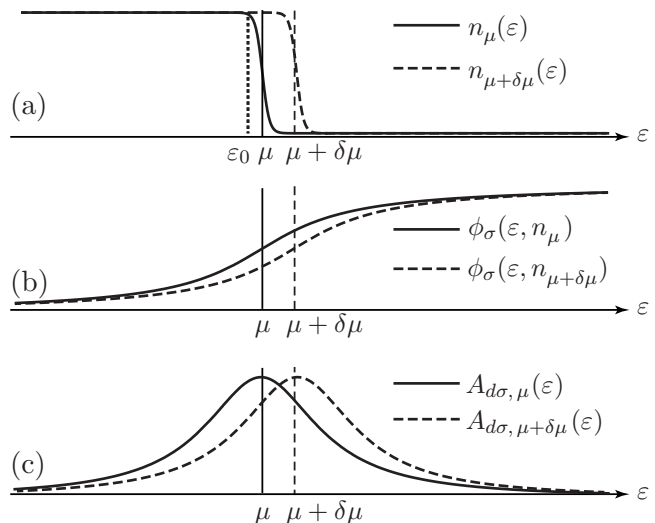


FIG. 4. Qualitative depiction of (a) the distribution function, (b) the phase shift and (c) the Kondo resonances in the impurity spectral function, for two choices of chemical potential, μ (solid lines) and $\mu + \delta\mu$ (dashed lines). Dotted lines illustrate the reference distribution function $n_{\varepsilon_0}^0(\varepsilon) = \theta(\varepsilon_0 - \varepsilon)$ in (a).

chemical potential only through the combination $\varepsilon - \mu$. In other words, if μ is changed to $\mu + \delta\mu$, e.g. by doping the system to increase the electron density, then the new phase shift at $\varepsilon + \delta\varepsilon$ equals the old one at ε ,

$$\delta_\sigma(\varepsilon + \delta\mu, n_{\mu+\delta\mu}) = \delta_\sigma(\varepsilon, n_\mu), \quad (13)$$

as illustrated in Fig. 4. [In fact, an alternative way to derive Eq. (12) is to impose Eq. (13), with the same ε_0 on both sides of the equation, as condition on the general phase shift expansion Eq. (11) for $\delta_\sigma(\varepsilon, n_\mu)$; the calculations are simplest if done at zero temperature, i.e. with $n_\mu \rightarrow n_{\mu_0}^0$.] Since at $T = 0$ the energy dependence of the phase shift determines that of the Kondo resonance in the impurity spectral function, $A_{d\sigma,\mu}(\varepsilon)$, the latter, too, is invariant under a simultaneous shift of ε and μ . Pictorially speaking, the “Kondo resonance floats on the Fermi sea” [13, 31]: if the Fermi surface rises, the Kondo resonance rises with it, and if the Fermi sea is deep enough (wide-band limit), the Kondo resonance does not change its shape while rising.

The next step is to express δ_0 and $\alpha_1 = \phi_1$ in terms of physical quantities, such as the local charge n_d and the local spin susceptibility χ_s . This can be done by calculating the latter quantities via the Friedel sum rule, evaluating the ground state phase shift in a small magnetic field. We discuss this in detail in the next section, in the more general context of the Anderson model. Here we just quote the results: for the Kondo model, one finds $\delta_0 = \pi/2$, $\alpha_1 = \phi_1 = \pi\chi_s$ and, since $\chi_s = 1/(4T_K)$, from Eq. (4), $E^* = T_K$ for the Fermi-liquid energy scale controlling the expansion Eq. (11).

Before proceeding further with the Anderson model, we wish to emphasize two important points:

- (i) We have restricted our attention to elastic scattering processes. As pointed out in Ref. [32], inelastic processes involve the difference between the energies of incoming and outgoing electrons and are therefore invariant under a global shift of all energies by $\delta\mu$.
- (ii) Eq. (11) corresponds to the first few terms of a general expansion of $\delta_\sigma(\varepsilon, n_{\sigma'})$ in powers of $\varepsilon - \varepsilon_0$ and $\int_{\varepsilon'} \delta n_{\sigma',\varepsilon_0}(\varepsilon')$. In the calculation of the conductance, for example at finite temperature, the α_1 and ϕ_1 terms give a vanishing linear contribution and must therefore be taken into account up to second order. To be consistent, one then needs to include the next subleading terms $\sim 1/T_K^2$ in the expansion of $\delta_\sigma(\varepsilon, n_{\sigma'})$. This has been worked out explicitly for the $SU(N)$ case with $N > 3$ [30–33, 46]. These subleading terms, however, turn out to vanish identically in the $SU(2)$ Kondo model, as a result of electron-hole symmetry. This is no longer the case for the asymmetric Anderson model, as we will see below.

B. Anderson model

The Anderson model is described by a low-energy Fermi-liquid fixed point for all regimes of parameters, hence we now seek to generalize the above approach to

this model, too. The main complication compared to the Kondo model is that the Anderson model involves an additional energy scale, namely the impurity level ε_d , and its physics depends in an essential way on the distance $\varepsilon_d - \mu_0$ between its impurity energy level and the chemical potential. We again Taylor expand the phase shift w.r.t. to a reference energy ε_0 , as in Eq. (11), but now include the next order in excitation energies [31]:

$$\begin{aligned} \delta_\sigma(\varepsilon, n_{\sigma'}) &= \delta_{0,\varepsilon_d-\varepsilon_0} + \alpha_{1,\varepsilon_d-\varepsilon_0}(\varepsilon - \varepsilon_0) \\ &- \phi_{1,\varepsilon_d-\varepsilon_0} \int_{\varepsilon'} \delta n_{\bar{\sigma},\varepsilon_0}(\varepsilon') + \alpha_{2,\varepsilon_d-\varepsilon_0}(\varepsilon - \varepsilon_0)^2 \\ &- \frac{1}{2} \phi_{2,\varepsilon_d-\varepsilon_0} \int_{\varepsilon'} (\varepsilon + \varepsilon' - 2\varepsilon_0) \delta n_{\bar{\sigma},\varepsilon_0}(\varepsilon') + \dots \end{aligned} \quad (14)$$

δ_0 , α_1 , ϕ_1 , α_2 and ϕ_2 are the Taylor coefficients of this expansion. In contrast to the case of the Kondo model, they now *do* depend explicitly on the reference energy ε_0 , and since we are in the wide-band limit, this dependence can arise only via the difference $\varepsilon_d - \varepsilon_0$. For notational simplicity, we will suppress this subscript below, taking this dependence to be understood. In the Kondo limit of Eq. (2), the dependence on ε_d drops out, and the coefficients δ_0 , α_1 , ϕ_1 , α_2 and ϕ_2 become universal, as seen in the previous section for δ_0 , α_1 and ϕ_1 .

Similarly to Sec. II A, the Taylor coefficients are not all independent as a result of the phase shift $\delta_\sigma(\varepsilon, n_{\sigma'})$ invariance under a change in ε_0 . Differentiating Eq. (14) w.r.t. ε_0 , and equating the coefficients of the various terms in the expansion (cst, $\sim (\varepsilon - \varepsilon_0)$, $\sim \int \delta n_{\bar{\sigma},\varepsilon_0}$) to zero, we therefore obtain the following three relations [47]:

$$-\delta'_0 - \alpha_1 + \phi_1 = 0, \quad (15a)$$

$$-\alpha'_1 - 2\alpha_2 + \phi_2/2 = 0, \quad (15b)$$

$$\phi'_1 + \phi_2 = 0. \quad (15c)$$

Here a prime denotes a derivative with respect to the energy argument, e.g. $\delta'_0 = d(\delta_{0,\varepsilon_d-\varepsilon_0})/d\varepsilon_d$.

As can be checked easily, Eqs. (15) guarantee that for any distribution $n_{\sigma'}$ with a well-defined chemical potential, e.g. n_μ , the phase shift $\delta_{\sigma,\varepsilon_d}(\varepsilon, n_\mu)$ (where the subscript ε_d indicates the ε_d dependence of its Fermi-liquid parameters) remains invariant if ε , ε_d and μ are all shifted by the same amount:

$$\delta_{\sigma,\varepsilon_d+\delta\mu}(\varepsilon + \delta\mu, n_{\mu+\delta\mu}) = \delta_{\sigma,\varepsilon_d}(\varepsilon, n_\mu). \quad (16)$$

Conversely, an alternative way to derive Eqs. (15) is to impose Eq. (16) as a condition on the Taylor expansion (14) for $\delta_{\sigma,\varepsilon_d}(\varepsilon, n_\mu)$.

Collecting results, the first order Fermi-liquid parameters, α_1 and ϕ_1 , are related to each other through

$$\phi_1 - \alpha_1 = \delta'_0, \quad (17)$$

while the second-order Fermi-liquid parameters, α_2 and ϕ_2 , can be expressed via Eqs. (15) in terms of derivatives

of lower-order ones:

$$\alpha_2 = -\frac{\delta_0''}{4} - \frac{3\alpha_1'}{4}, \quad \phi_2 = -\phi_1'. \quad (18)$$

Having established the above relations between the Fermi-liquid parameters, we henceforth choose the reference energy at the zero-temperature chemical potential, $\varepsilon_0 = \mu_0$. Moreover, since the choice of μ_0 is arbitrary in the wide-band limit, we henceforth set $\mu_0 = 0$. Hence, the energy argument of the Fermi-liquid parameters is henceforth understood to be ε_d , i.e. δ_0 stands for δ_{0,ε_d} , etc.

C. Charge and spin static susceptibilities

Our next task is to express the Fermi liquid parameters in terms of physical quantities. This can be done using the Friedel sum rule. To this end, consider a zero-temperature system in a small nonzero magnetic field, B , with distribution $n_{\mu_{\sigma'}}^0(\varepsilon') = \theta(\mu_{\sigma'} - \varepsilon')$ and spin-split chemical potentials, $\mu_{\sigma'} = \sigma'B/2$, as illustrated in Fig. 5. Using this distribution for $n_{\sigma'}$ in Eq. (14), with $\varepsilon_0 = 0$ and $\delta n_{\bar{\sigma},0} = n_{\mu_{\bar{\sigma}}}^0 - n_0^0$, we find:

$$\delta_\sigma(\varepsilon, n_{\mu_{\sigma'}}^0) = \delta_0 + \alpha_1 \varepsilon - \frac{\phi_1}{2} \bar{\sigma} B + \alpha_2 \varepsilon^2 - \frac{\phi_2}{2} [\varepsilon \bar{\sigma} B/2 + B^2/8]. \quad (19)$$

Now evoke the Friedel sum rule [48]. For given spin σ it relates the average charge bound by the impurity at $T = 0$, $n_{d\sigma} = \langle \hat{n}_{d\sigma} \rangle$, to the ground state phase shift at

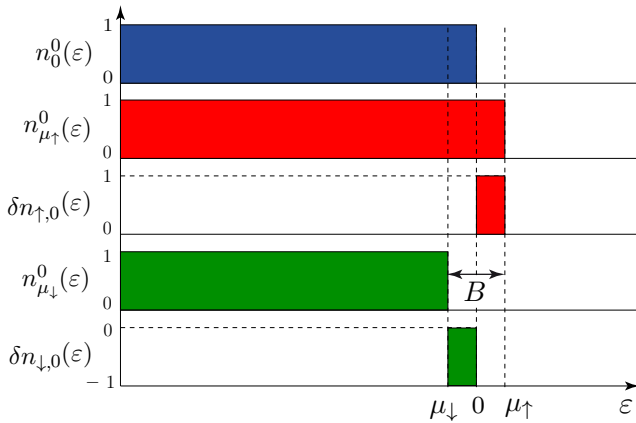


FIG. 5. Zero-temperature quasiparticle distribution functions used for the calculation of Eq. (19): At zero field we use n_0^0 as reference distribution (in Sec. II C, we set $\varepsilon_0 = \mu_0 = 0$), while the system at small field B has distribution $n_{\mu_{\sigma'}}^0$, differing from the reference distribution by $\delta n_{\sigma,0} = n_{\mu_{\sigma}}^0 - n_0^0$. The shifted chemical potentials, $\mu_{\sigma} = \sigma B/2$, derive from the condition $\langle b_{\varepsilon\sigma}^\dagger b_{\varepsilon\sigma} \rangle = 0$ for $\varepsilon - \sigma B/2 > 0$.

the chemical potential, i.e. at $\varepsilon = \mu_{\sigma}$:

$$\pi n_{d\sigma} = \delta_\sigma(\mu_{\sigma}, n_{\mu_{\sigma'}}^0) \quad (20a)$$

$$= \delta_0 + \frac{\sigma}{2}(\alpha_1 + \phi_1)B + \frac{1}{4}(\alpha_2 + \phi_2/4)B^2. \quad (20b)$$

Thus, the average local charge n_d and average magnetization m_d of the local level can be expressed as:

$$n_d = n_{d\uparrow} + n_{d\downarrow} = \frac{2\delta_0}{\pi} + \frac{1}{2\pi}(\alpha_2 + \phi_2/4)B^2, \quad (21a)$$

$$m_d = (n_{d\uparrow} - n_{d\downarrow})/2 = \frac{B}{2\pi}(\alpha_1 + \phi_1). \quad (21b)$$

In the strong-coupling Kondo regime we have $n_d = 1$ at zero field, implying $\delta_0 = \pi/2$. In general, however, $n_{d\sigma}$ is a function of ε_d . From Eqs. (21), the local charge and spin susceptibilities at zero field are given by

$$\chi_c = -\left. \frac{\partial n_d}{\partial \varepsilon_d} \right|_{B=0} = -2\frac{\delta_0'}{\pi} = \frac{2}{\pi}(\alpha_1 - \phi_1), \quad (22a)$$

$$\chi_s = \left. \frac{\partial m_d}{\partial B} \right|_{B=0} = \frac{1}{2\pi}(\alpha_1 + \phi_1). \quad (22b)$$

Using Eqs. (22a) and (22b), the Fermi-liquid parameters can be written in terms of the charge and spin susceptibilities χ_c and χ_s , and their derivatives w.r.t. to ε_d , denoted by χ_c' and χ_s' . The result is given in Eq. (5) in the introduction. As a consistency check, we note from Eq. (5) that $(\alpha_2 + \phi_2/4)/\pi = -\chi_s'$, thus Eqs. (21) imply

$$\frac{\partial n_d}{\partial B} = -\frac{\partial m_d}{\partial \varepsilon_d}, \quad (23)$$

which is a standard thermodynamic identity.

For the Anderson model, n_d , χ_c , χ_s and their derivatives w.r.t. ε_d can all be computed using the Bethe Ansatz, see Appendix A. This allows us to explicitly determine how the Fermi-liquid parameters depend on ε_d . A corresponding plot is shown in Fig. 2 for $U/\Delta = 5$.

Since χ_c , χ_s , χ_c' and χ_s' all depend on three independent variables (Δ , and the dimensionless ratios ε_d/U and ε_d/Δ), the low energy behavior can no longer be characterized in terms of a single energy scale. Nevertheless, to define the Fermi-liquid transport coefficients c_T , c_V and c_T in Eq. (6), we need to define a single characteristic scale, E^* . Somewhat arbitrarily, we choose $E^* = \pi/(4\alpha_1)$, as stated in Eq. (4). However, we emphasize that away from the strong-coupling Kondo limit, E^* can no longer be associated with the Kondo temperature (which is not defined in the mixed-valence and empty-orbital regimes, anyway).

The Anderson model has a particle-hole symmetry, which manifests itself as an invariance under the replacements $\varepsilon_d \rightarrow -\varepsilon_d - U$ for the impurity single-particle energy and $n_d \rightarrow 2 - n_d$ for the impurity charge. The particle-hole symmetric point therefore corresponds to $\varepsilon_d = -U/2$ and $n_d = 1$. Moreover, χ_c and χ_s are symmetric with respect to particle-hole symmetry, while χ_c' and χ_s' are antisymmetric. Consequently, Eqs. (5) show

that α_1 and ϕ_1 are symmetric while α_2 and ϕ_2 are antisymmetric, a feature already pointed out in the introduction. As a result, α_2 and ϕ_2 identically vanish at the particle-hole symmetric point $\varepsilon_d = -U/2$. At this point, our result for the current will therefore agree with those of Refs. [13, 19, 23, 24]. In the Kondo limit of Eq. (2), charge fluctuations are suppressed such that $\chi_c = 0$, and Eq. (22a) reproduces the Fermi-liquid identity Eq. (12) of the Kondo model.

Let us now establish contact with previous works. The Friedel sum rule implies an impurity-induced change in density of states per spin species given by $\nu_{\sigma,\text{imp}} = (1/\pi)\partial_\varepsilon\delta_\sigma(\varepsilon, n_{\mu_0}^0)|_{\varepsilon=\mu_0} = \alpha_1/\pi$, and hence a corresponding impurity-induced change in the specific heat of $\gamma_{\text{imp}} = (\pi^2 k_B^2/3) \sum_\sigma \nu_{\sigma,\text{imp}} = (2\pi k_B^2/3)\alpha_1$, where k_B denotes the Boltzmann constant. Eliminating ϕ_1 from Eqs. (22), we find

$$\frac{4\chi_s}{(g\mu_B)^2} + \chi_c = \frac{4\alpha_1}{\pi} = \frac{6\gamma_{\text{imp}}}{\pi^2 k_B^2}, \quad (24)$$

where physical units have been reinstated (only in this equation) by replacing χ_s by $\chi_s/(g\mu_B)^2$. This relation agrees with previous Fermi-liquid studies [3, 14, 20]. Next, consider the Wilson ratio R , defined as the ratio of the impurity contributions to the spin susceptibility and specific heat, χ_s and γ_{imp} , relative to their respective bulk contributions, $\chi_{s,\text{bulk}} = \nu_0/2$ and $\gamma_{\text{bulk}} = (\pi^2 k_B^2/3)2\nu_0$, where ν_0 is the bulk density of states per spin species. Eq. (24) implies

$$R \equiv \frac{\chi_s/\chi_{s,\text{bulk}}}{\gamma_{\text{imp}}/\gamma_{\text{bulk}}} = \frac{2}{1 + \chi_c/(4\chi_s)}, \quad (25)$$

in agreement with Ref. [20]. This interpolates between the non-interacting case, where the charge and spin susceptibilities are trivially related by $\chi_s = \chi_c/4$, hence $R = 1$, and the Kondo limit, where $\chi_c = 0$, hence $R = 2$.

So far in this section, we have not used the specific form of the Anderson model. The only ingredients that we have used are the presence of a single-particle energy ε_d for the impurity and the assumption of Fermi-liquid behaviour. This emphasizes the generality of our Fermi-liquid approach, which is also applicable, for instance, to other impurity models such as the interacting resonant model.

D. Analytical expressions

In order to better understand the dependence of the Fermi-liquid parameters on ε_d , it is instructive to consider certain limiting cases where analytical expressions can be derived. In the Kondo regime, $U \gg \Delta$ and $-U + \Delta < \varepsilon_d < -\Delta$, spin excitations dominate and the charge susceptibility can be neglected ($\chi_c \simeq 0$, $\chi'_c \simeq 0$), so that [from Eqs. (5)]

$$\alpha_1 \simeq \phi_1 \simeq \pi\chi_s, \quad 4\alpha_2/3 \simeq \phi_2 \simeq -\pi\chi'_s. \quad (26)$$

The spin susceptibility is given with a very good accuracy by the asymptotical expression (see Appendix A)

$$\chi_s = \frac{1}{2\sqrt{2U\Delta}} e^{\pi(U/8\Delta - \Delta/2U)} e^{-x^2}, \quad (27)$$

where we introduced the distance to the particle-hole symmetric point $x = (\varepsilon_d + U/2)\sqrt{\pi/(2\Delta U)}$. Eq. (27) agrees with the well-known formula $1/T_K \propto (U\Delta)^{-1/2} e^{-\pi\varepsilon_d(\varepsilon_d+U)/(2\Delta U)}$ [35], up to an extra factor $e^{-\pi\Delta/(2U)}$, which was neglected in [35] because the limit $U/\Delta \gg 1$ is implicit there. Differentiating Eq. (27) w.r.t. ε_d , we find

$$-\chi'_s = \frac{\pi^{1/2}}{2\Delta U} e^{\pi(U/8\Delta - \Delta/2U)} x e^{-x^2}. \quad (28)$$

Eqs. (26) to (28) together largely explain the shape of all the curves in Fig. 2, namely approximately Gaussian for α_1 and ϕ_1 , or the derivative of a Gaussian for α_2 and ϕ_2 .

The other limit in which analytical expressions can be derived is the empty-orbital regime, for $\varepsilon_d \gg \Delta$. The results are detailed in Appendix B. Together with Eqs. (27) and (28), they give us a good analytical understanding of the ε_d dependence of the Fermi-liquid parameters. In the Kondo regime, α_1 and ϕ_1 follow the spin susceptibility (or the inverse Kondo temperature) and decrease with increasing ε_d (for $\varepsilon_d > -U/2$) while crossing over into the mixed-valence regime. Finally, in the empty-orbital regime $\chi_s = \chi_c/4$, hence α_1 still follows the spin susceptibility, but with a factor 2, $\alpha_1 \simeq 2\pi\chi_s$, while ϕ_1 becomes negligible.

It is interesting to consider the ratios α_2/α_1^2 and ϕ_2/α_1^2 which measure the importance of the second generation of Fermi parameters compared to the first one. In the Kondo region but far enough from particle-hole symmetry, $\alpha_2 \sim \phi_2 \sim 1/(T_K\Delta)$ [the precise formula is implied by Eq. (28)] so that $\alpha_2/\alpha_1^2 \sim \phi_2/\alpha_1^2 \sim T_K/\Delta$. The two ratios are small but increase with ε_d and T_K towards the mixed-valence region where they reach values of order 1. Above, in the empty-orbital region, $\varepsilon_d \gg \Delta$, $\phi_2/\alpha_1^2 = 6/\pi$ for $\varepsilon_d \ll U$ but is negligible for $\varepsilon_d \gg U$, while $\alpha_2/\alpha_1^2 = \varepsilon_d/\Delta$ continues to increase with ε_d [see Eqs. (B6) to (B8)].

E. Hamiltonian form

The analysis carried out so far may seem abstract. It is based on the elastic phase shift alone and it is not clear how transport quantities and other observables can be computed. We thus need to write an explicit low-energy Hamiltonian reproducing the phase shift of Eq. (14). The leading order, or strong coupling Hamiltonian, is simply given by the first term of Eq. (3),

$$H_0 = \sum_\sigma \int d\varepsilon (\varepsilon - \sigma B/2) b_{\varepsilon\sigma}^\dagger b_{\varepsilon\sigma}, \quad (29)$$

where the quasiparticle operators $b_{\varepsilon\sigma}$, defined in the introduction, satisfy the fermionic anticommutation relations

$$\{b_{\varepsilon\sigma}, b_{\varepsilon'\sigma'}^\dagger\} = \delta_{\sigma,\sigma'}\delta(\varepsilon - \varepsilon'), \quad \{b_{\varepsilon\sigma}, b_{\varepsilon'\sigma'}\} = 0. \quad (30)$$

The low-energy Hamiltonian admits an expansion in correspondence with the phase shift expansion [49] of Eq. (14), the increasing orders being increasingly irrelevant in the renormalization group sense [42]. The first two terms of this expansion are given in Eq. (3).

The computation of the elastic phase shift with H involves all processes stemming from H_0 and H_α , in addition to the Hartree diagrams inherited from H_ϕ . Using $\delta_\sigma(\varepsilon)/\pi = \varepsilon - \sigma B/2 - \partial\langle H_{\text{FL}}\rangle/\partial n_\sigma(\varepsilon)$, it is straightforward to check that Eq. (14) is reproduced, as required.

In Eq. (3), H_α describes purely elastic scattering of the lead electrons by the Anderson impurity at $\mathbf{r} = 0$. Its structure coincides with the first two terms of a low-energy expansion for a resonant level model. When the resonant level is centered at zero energy, one has $\alpha_2 = 0$ in agreement with our findings that α_2 vanishes at particle-hole symmetry. In addition, one then has $\alpha_1 \sim \chi_s \sim 1/T_K$, and T_K is interpreted as the width of the resonant level. In the general case however, the Kondo resonance is centered off the Fermi energy and $\alpha_2 \neq 0$.

The interaction term H_ϕ is the reminder that the resonance has a many-body origin. Pairs of electrons with opposite spins interact locally, at $\mathbf{r} = 0$, through polarization of the ground state singlet. The combination $\phi_1 + \phi_2\varepsilon$ can be understood as the low-energy expansion of the corresponding vertex. Note that local parallel spin interaction is forbidden by the Pauli principle (otherwise we would have a product of identical annihilation operators in H_ϕ). Note that the α_2 and ϕ_2 terms exhaust all the possible operators of dimension 3 respecting spin symmetry [31].

To summarize this section, Eq. (3) constitute a rigorous and exact low-energy Hamiltonian for the Anderson model (or for other similar models), and a basis for computing the low-energy quadratic behaviour of observables. We shall use it in the next section to compute the conductance. The introduction of the elastic phase shift was mainly aimed at determining the expressions of the Fermi-liquid parameters given in Eq. (5).

III. CURRENT CALCULATION

The Fermi liquid theory developed so far is very general, and applies to many quantum impurity systems with a Fermi liquid ground state and a single relevant channel of spinful electrons attached to it. We now turn to the concrete case of the Anderson model and calculate the current through a quantum dot using the Fermi-liquid theory described in the previous section. Similar current calculations can be found in Refs. [17, 30, 32]. Sec. III A introduces the Anderson model and the corresponding

Fermi-liquid Hamiltonian valid at low energy, already outlined in the Introduction. The current operator is given in Sec. III B and expanded over the convenient basis of quasiparticle states. The perturbative calculation of the current is then separated into the elastic part in Sec. III C and the inelastic part in Sec. III D.

A. Hamiltonians

1. Anderson model

We consider the model of a single-level dot symmetrically coupled to right and left leads with the Hamiltonian $H = H_a + H_{\text{AM}}$, with $H_a = \sum_\sigma \int d\varepsilon \varepsilon a_{\varepsilon\sigma}^\dagger a_{\varepsilon\sigma}$ and

$$H_{\text{AM}} = \sum_\sigma \int d\varepsilon \varepsilon \tilde{b}_{\varepsilon\sigma}^\dagger \tilde{b}_{\varepsilon\sigma} + \varepsilon_d \sum_\sigma n_\sigma + U \hat{n}_{d\uparrow} \hat{n}_{d\downarrow} + \sqrt{\nu_0} t \sum_\sigma \int d\varepsilon \left(\tilde{b}_{\varepsilon\sigma}^\dagger d_\sigma + d_\sigma^\dagger \tilde{b}_{\varepsilon\sigma} \right), \quad (31)$$

where, instead of the original left and right operators, $c_{L,\varepsilon\sigma}$ and $c_{R,\varepsilon\sigma}$, we use the symmetric and antisymmetric combinations

$$\begin{pmatrix} \tilde{b}_{\varepsilon\sigma} \\ a_{\varepsilon\sigma} \end{pmatrix} = \frac{1}{\sqrt{2}} \begin{pmatrix} 1 & 1 \\ 1 & -1 \end{pmatrix} \begin{pmatrix} c_{L,\varepsilon\sigma} \\ c_{R,\varepsilon\sigma} \end{pmatrix}. \quad (32)$$

These satisfy the same anticommutation relations as in Eq. (30). The leads are approximated by a linear spectrum with a constant density of states ν_0 per spin species. d_σ is the electron operator of the dot and $n_\sigma = d_\sigma^\dagger d_\sigma$ the corresponding density for spin σ . $U > 0$ denotes the charging energy, ε_d the single-particle energy on the dot and t the tunneling matrix element from the dot to the symmetric combination of leads. The antisymmetric combination $a_{\varepsilon\sigma}$, associated with the wavefunction

$$\psi_{k\sigma}^a(x) = \left(e^{i(k_F+k)x} - e^{-i(k_F+k)x} \right) / \sqrt{2} \quad (33)$$

for all x , decouples from the dot variables. Here $x < 0$ describes the left lead and $x > 0$ the right lead, energies and wavevectors are related through $\varepsilon = \hbar v_F k$. For simplicity, the whole system is assumed to be one-dimensional. Being odd in x , this wavefunction vanishes at the origin and is therefore not affected by the Anderson impurity. We define the hybridization $\Delta = \pi \nu_0 t^2$ for later use.

2. Effective low-energy Hamiltonian

At low energy, screening takes place and the Anderson model flows to a Fermi-liquid fixed point for all values of ε_d , U and Δ . The Hamiltonian describing the low-energy physics of Eq. (31) is then given by $H_a + H_{\text{FL}}$, with the Fermi-liquid Hamiltonian H_{FL} for the even channel given by Eq. (3).

The difference between the original operators $\tilde{b}_{\varepsilon\sigma}$ and the quasiparticle operators $b_{\varepsilon\sigma}$ is the zero-energy phase shift δ_0 , i.e. the phase shift that arises for $H_\alpha = H_\phi = 0$. Hence $b_{\varepsilon\sigma}$ is associated with the scattering state

$$\psi_{k\sigma}^b(x) = \begin{cases} (e^{i(k_F+k)x} - \mathcal{S}_0 e^{-i(k_F+k)x})/\sqrt{2} & x < 0, \\ (e^{-i(k_F+k)x} - \mathcal{S}_0 e^{i(k_F+k)x})/\sqrt{2} & x > 0, \end{cases} \quad (34)$$

with the S-matrix $\mathcal{S}_0 = e^{2i\delta_0}$.

B. Current operator

In a one-dimensional geometry, the local current operator is given by

$$\hat{I}(x) = \frac{e\hbar}{2mi} \sum_{\sigma} (\psi_{\sigma}^{\dagger}(x) \partial_x \psi_{\sigma}(x) - \partial_x \psi_{\sigma}^{\dagger}(x) \psi_{\sigma}(x)) \quad (35)$$

where m is the electron mass. Various expressions for the current can be derived depending on which basis of states it is expanded in. Here we choose a basis adapted to the low-energy model, namely we expand over the zero-energy scattering states

$$\psi_{\sigma}(x) = \int d\varepsilon \sqrt{\nu_0} [\psi_{k\sigma}^a(x) a_{\varepsilon\sigma} + \psi_{k\sigma}^b(x) b_{\varepsilon\sigma}] \quad (36)$$

with $\nu_0 = 1/hv_F$ the density of states of incoming quasiparticles.

A voltage bias applied between the two leads, $\mu_L - \mu_R = eV$, drives a current through the quantum dot. In a stationary situation, the current is conserved along the one-dimensional space. We thus define the symmetric current operator as $\hat{I} = (\hat{I}(x) + \hat{I}(-x))/2$, where x is arbitrary, corresponding to the average of the left and right currents. Inserting the expansion Eq. (36) in Eq. (35), one finds the Landauer-Buttiker [50] type current expression

$$\hat{I} = \frac{e}{2\hbar} \sum_{\sigma} \int_{\varepsilon, \varepsilon'} a_{\varepsilon\sigma}^{\dagger} b_{\varepsilon'\sigma} \left(e^{i(k'-k)x} - \mathcal{S}_0 e^{-i(k'-k)x} \right) + \text{h.c.}, \quad (37)$$

with $x < 0$. A more compact expression can be obtained with the definition $a_{\sigma}(x) \equiv \int d\varepsilon a_{\varepsilon\sigma} e^{ikx}$, namely

$$\hat{I} = \frac{e}{2\hbar} \sum_{\sigma} (a_{\sigma}^{\dagger}(x) b_{\sigma}(x) - a_{\sigma}^{\dagger}(-x) (\mathcal{S}_0 b_{\sigma})(-x) + \text{h.c.}). \quad (38)$$

Physically, operators taken at x ($-x$) correspond here to incoming (outgoing) states.

C. Elastic scattering

We study the average current through the dot in the presence of a voltage bias. We include in this section only the elastic and Hartree contributions, the inelastic terms will be considered in the next Sec. III D.

1. Strong coupling fixed point

We start by considering the strong coupling fixed point, i.e. without the Fermi-liquid corrections H_α and H_ϕ , where we have a free gas of quasiparticles. The Hamiltonian is $H_0 + H_a$ and $a_{\varepsilon\sigma}^{\dagger}$ and $b_{\varepsilon'\sigma}^{\dagger}$ create eigenstates of the model. The left and right scattering states, which are even and odd combinations of $a_{\varepsilon\sigma}$ and $b_{\varepsilon'\sigma}$, are in thermal equilibrium with spin-dependent chemical potentials $\mu_{L\sigma} = \mu_L + \sigma B/2$ and $\mu_{R\sigma} = \mu_R + \sigma B/2$. Hence, we have

$$\begin{aligned} \langle a_{\varepsilon\sigma}^{\dagger} a_{\varepsilon'\sigma'} \rangle &= \langle b_{\varepsilon\sigma}^{\dagger} b_{\varepsilon'\sigma'} \rangle = \delta_{\sigma,\sigma'} \delta(\varepsilon - \varepsilon') \frac{f_{L\sigma}(\varepsilon) + f_{R\sigma}(\varepsilon)}{2} \\ \langle a_{\varepsilon\sigma}^{\dagger} b_{\varepsilon'\sigma'} \rangle &= \delta_{\sigma,\sigma'} \delta(\varepsilon - \varepsilon') \frac{f_{L\sigma}(\varepsilon) - f_{R\sigma}(\varepsilon)}{2} \end{aligned} \quad (39)$$

with the Fermi distributions $f_{L\sigma}(\varepsilon)$ and $f_{R\sigma}(\varepsilon)$. The mean value of the current \hat{I} is then given by

$$I = \langle \hat{I} \rangle = \frac{e}{h} \sum_{\sigma} \int d\varepsilon \mathcal{T}_{\sigma}(\varepsilon) [f_{L\sigma}(\varepsilon) - f_{R\sigma}(\varepsilon)] \quad (40)$$

with the transmission $\mathcal{T}_{\sigma}(\varepsilon) = \sin^2(\delta_0)$, which here is energy- and spin-independent, because H_α and H_ϕ have been neglected. Performing the summation over ε , one finds the average current $I = (2e^2 V/h) \sin^2(\delta_0)$, which is maximal (unitary) at particle-hole symmetry $\delta_0 = \pi/2$ and approaches zero as $|\varepsilon_d - U/2|/\Delta$ becomes very large, so that $|\delta_0| \rightarrow 0$.

2. Elastic scattering and phase shift

We now include the Fermi-liquid terms H_α and H_ϕ into the Hamiltonian. We first consider the elastic scattering processes associated with H_α . Since they describe single-particle processes, they can be absorbed in H_0 by a change of scattering basis. The above analysis for computing the current can be reproduced with the only change that the \mathcal{S} matrix now carries an energy and spin dependence, $\mathcal{S}_{\sigma}(\varepsilon) = e^{2i\delta_{\sigma}(\varepsilon)}$, and the knowledge of the phase shift $\delta_{\sigma}(\varepsilon)$ suffices to characterize elastic scattering. The resulting current is still given by Eq. (40), with $\mathcal{T}_{\sigma}(\varepsilon) = \sin^2[\delta_{\sigma}(\varepsilon)]$.

Before writing the expression of the elastic phase shift, we note that the Hartree terms stemming from H_ϕ are formally equivalent to elastic scattering. Diagrammatically, each interaction vertex connecting a fermionic line to a single closed fermionic loop (a bubble) is similar to a local potential vertex where the energy is conserved after scattering. As mentioned already earlier, collecting purely elastic and Hartree contributions, and calculating the phase shift, we indeed arrive at Eq. (14).

For the rest of this section, we set $B = 0$. At finite temperature T and voltage V , the energy integrals in the

phase shift expansion Eq. (14) yield

$$\int_{\varepsilon} \delta n_{\sigma,0}(\varepsilon) = 0, \quad \int_{\varepsilon} \varepsilon \delta n_{\sigma,0}(\varepsilon) = \frac{(\pi T)^2}{6} + \frac{(eV)^2}{8}, \quad (41)$$

so that we obtain the spin-independent phase shift

$$\delta_{\sigma}(\varepsilon) = \delta_0 + \alpha_1 \varepsilon + \alpha_2 \varepsilon^2 - \phi_2 \left(\frac{(\pi T)^2}{12} + \frac{(eV)^2}{16} \right). \quad (42)$$

Inserting this result into Eq. (40) for the elastic current and expanding to third order in energy, one obtains

$$I_{\text{el}} = \frac{2e^2 V}{h} \left[\sin^2 \delta_0 - \sin 2\delta_0 \phi_2 \left(\frac{(\pi T)^2}{12} + \frac{(eV)^2}{16} \right) + (\alpha_2 \sin 2\delta_0 + \alpha_1^2 \cos 2\delta_0) \left(\frac{(\pi T)^2}{3} + \frac{(eV)^2}{12} \right) \right]. \quad (43)$$

This represents the elastic and Hartree contributions to the current.

D. Inelastic scattering

In the previous section, only the Hartree diagrams associated to H_{ϕ} and the terms H_{α} have been included in the current calculation. A full account of H_{ϕ} requires the use of the Keldysh framework [51] to compute the current in an out-of-equilibrium setting. The average current is given by

$$I = \langle T_c \hat{I}(t) e^{-\frac{i}{\hbar} \int_c dt' : H_{\phi} : (t')} \rangle, \quad (44)$$

where $: H_{\phi} :$ denotes the interaction terms H_{ϕ} in Eq. (3), with the Hartree contributions removed and incorporated in the scattering wave functions and operators appearing in H_0 . The Keldysh contour \mathcal{C} runs along the forward time direction on the branch $\eta = +$ followed by a backward evolution on the branch $\eta = -$, and T_c is the corresponding time ordering operator. Time evolution and mean values are determined by the free Hamiltonian H_0 , Eq. (29), now incorporating all elastic and Hartree processes. Hence the current operator is given by Eq. (38) with \mathcal{S}_0 simply replaced by the energy-dependent $\mathcal{S}_{\sigma}(\varepsilon)$. Starting with Eq. (44), we expand to second order in $: H_{\phi} :$, and compute the resulting integrals in Keldysh space. The first order term vanishes by construction, and the only remaining second-order term is shown in Fig. 6. The resulting current contribution is [32]

$$I_{\text{inel}} = \frac{2e^2 V}{h} \phi_1^2 \cos 2\delta_0 \left(\frac{2(\pi T)^2}{3} + \frac{5(eV)^2}{12} \right). \quad (45)$$

Terms proportional to $\sim \phi_1 \phi_2$ and $\sim \phi_2^2$ are not included here, since they involve higher powers of T and/or eV . The total average current is obtained by summing the elastic and inelastic terms, $I = I_{\text{el}} + I_{\text{inel}}$.

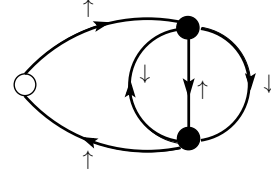


FIG. 6. This diagram represents an inelastic process in which an electron is scattered and locally excites an electron-hole pair.

IV. FERMI-LIQUID TRANSPORT COEFFICIENTS

In this section, we discuss the results for the current obtained at low energy in terms of Fermi-liquid transport coefficients c_B , c_T and c_V introduced in Eq. (6).

A. Finite magnetic field

In principle, the set of Fermi-liquid parameters derived above is not essential for the calculation of the linear conductance at zero temperature and finite magnetic field. In this regime, the ground state is still a Fermi liquid, even at large magnetic field. Moreover, although a finite magnetic field separates the chemical potentials of the two spin orientations, $\mu_{\sigma} = \sigma B/2$, it does not create room for particle-hole excitations (a term of order V^3 at least is necessary for particle-hole excitations). Thus, the linear conductance is given by Eq. (40), which reduces to

$$G = \frac{e^2}{h} \sum_{\sigma} \sin^2[\delta_{\sigma}(\varepsilon = \mu_{\sigma})]. \quad (46)$$

The phase shifts occurring herein are related via the Friedel sum rule, Eq. (20a), to the spin-dependent populations, $\delta_{\sigma}(\mu_{\sigma}) = \pi n_{d\sigma}$. These are static observables that can be computed directly from Bethe-Ansatz or NRG techniques, hence Eq. (46) can be evaluated without resorting to our Fermi-liquid expansion of the phase shift.

We may nevertheless use the latter to compute the low-field expansion of the linear conductance, as given by Eq. (6), in order to compare c_B with c_T and c_V . Substituting the small-field Fermi-liquid expansion Eq. (20b) for $\delta_{\sigma}(\mu_{\sigma})$ into Eq. (46) and expanding in B we obtain the Fermi-liquid coefficient c_B given in Eq. (7). This Fermi liquid expression interpolates continuously between the empty-orbital Eq. (8) and Kondo limits Eq. (10).

B. Finite temperature and non-linear conductance

Since the definition of the Fermi liquid scale is somewhat arbitrary, there is no unambiguous way to define the Fermi-liquid transport coefficients c_T and c_V in the general case. Here we use the definition of Eq. (6) with

the Fermi-liquid scale E^* defined in Eq. (4), which recovers conventional results in the particle-hole Kondo limit where $E^* = T_K$. The current obtained in the previous section then yields the Fermi-liquid transport coefficients

$$c_T = \frac{\pi^4}{16} \frac{\left(\frac{\phi_2}{12} - \frac{\alpha_2}{3}\right) \sin 2\delta_0 - \left(\frac{\alpha_1^2}{3} + \frac{2\phi_1^2}{3}\right) \cos 2\delta_0}{\alpha_1^2}, \quad (47)$$

and

$$c_V = \frac{\pi^2}{64} \frac{\left(\frac{3\phi_2}{4} - \alpha_2\right) \sin 2\delta_0 - (\alpha_1^2 + 5\phi_1^2) \cos 2\delta_0}{\alpha_1^2}. \quad (48)$$

At particle-hole symmetry, these expressions simplify since $\alpha_2 = 0$, $\phi_2 = 0$ and $\delta_0 = \pi/2$. They can be written in terms of the Wilson ratio, $R = 1 + \phi_1/\alpha_1$ [from Eq. (25)], namely $c_T = (\pi^4/48)[1 + 2(R-1)^2]$ and $c_V = (\pi^2/64)[1 + 5(R-1)^2]$. Their ratio is thus given by

$$\frac{c_V}{c_T} = \frac{3}{4\pi^2} \frac{1 + 5(R-1)^2}{1 + 2(R-1)^2}, \quad (49)$$

in agreement with Refs. [19, 34, 52]; it interpolates between $3/(2\pi^2)$ in the Kondo limit $R \rightarrow 2$ and $3/(4\pi^2)$ in the non-interacting limit $R \rightarrow 1$. The values of c_T and c_V in the Kondo regime are given in Eqs. (9). In the non-interacting limit, $U = 0$, i.e. for the resonant level model, the FL transport coefficients are readily calculated. One obtains $c_B = \pi^2/64$ and the ratio $c_V/c_T = 3/(4\pi^2)$ for all values of ε_d .

V. NUMERICAL RESULTS AND DISCUSSION

In the previous sections, we developed a quasiparticle Fermi-liquid theory of the Anderson model. In its generic form, this Fermi-liquid theory necessarily includes four Fermi-liquid parameters in addition to the phase shift. We used this Fermi-liquid theory to compute the conductance through a symmetrically coupled quantum dot, and determined the Fermi-liquid transport coefficients, c_V , c_T , and c_B , defined in Eq. (6). As we have shown in Section II C (already summarized in Eqs. (5) of the Introduction), the only inputs needed to compute the Fermi-liquid coefficients, – and thus the transport coefficients from Eqs. (7), (47) and (48), – are the spin (χ_s) and charge (χ_c) susceptibilities and their derivatives. We obtained these susceptibilities via two complementary methods: the Bethe Ansatz solution, discussed in Appendix A, and through numerical renormalization group calculations [53]. Extracting the Fermi-liquid parameters from χ_s and χ_c , we were then able to compute the transport coefficients in terms of the bare parameters of the Anderson model.

The results for c_B , c_T and c_V were already advertised and plotted in Fig. 3 of the Introduction for $U/\Delta = 10$. The dependence of c_V on the ratio U/Δ is presented in Fig. 7. For $U/\Delta \lesssim 2$, the ε_d dependence of the coefficient

c_V is almost the same as predicted by a non-interacting resonant level model. We remark that in this weakly interacting limit NRG is apparently less accurate than for stronger interactions. This is a consequence of NRG's logarithmic discretization scheme and its reduced accuracy for non-interacting systems. Notice that even in this simple limit, c_V does depend on the position of the resonant level, since the slope and the curvature of the local density of states both vary with the position of the level, ε_d . Increasing the ratio U/Δ further, a local-moment regime develops around $\varepsilon_d + U/2 \approx 0$ for $U/\Delta \gtrsim 10$, where the value of the transport coefficients is approximately given by Eqs. (9) and (10). The size of the Kondo region (plateau) increases with U/Δ , while the crossovers from the Kondo to the empty-orbital regimes occur over the energy scale Δ . As mentioned already in the In-

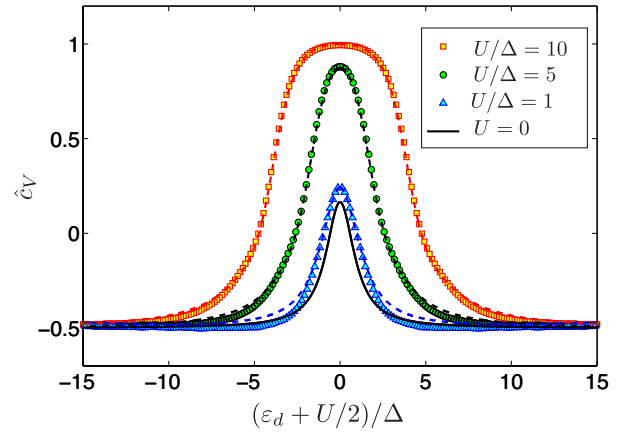


FIG. 7. (Color online) The transport Fermi-liquid coefficient $\hat{c}_V = c_V/(3\pi^2/32)$ as a function of $(\varepsilon_d + U/2)/\Delta$ for different values of U/Δ , using Bethe Ansatz (lines) and numerical renormalization group (symbols) calculations.

roduction, the crossover from the Kondo regime to the empty-orbital regime becomes universal in the $U \rightarrow \infty$ limit. To demonstrate this, we define the energy ε_d^* as the single-particle energy for which the impurity occupancy is $\langle \hat{n}_d \rangle = 1/2$, and reproduce Fig. 7 in Fig. 8, but with the single-particle energy ε_d measured relative to ε_d^* , and normalized by Δ . Clearly, c_V rapidly approaches a universal crossover curve, $c_V = f_V(\frac{\varepsilon_d - \varepsilon_d^*}{\Delta})$ as the interaction is increased. The scaling limit $U \rightarrow \infty$ can be accessed directly in the Bethe Ansatz solution. In this case, the susceptibilities χ_c and χ_s have integral representations (see Eqs. (A13) and (A14) in Appendix A), which can be used to compute the scaling curves shown as continuous black lines in Fig. 8. The transport coefficients c_T and c_B exhibit similar scaling properties, shown in the lower two panels of Figs. 8.

The transport coefficients c_V , c_T , and c_B are of immediate experimental significance. Nevertheless, extracting their *absolute value* in a quantum dot experiment is not very straightforward since, to do that, one should first

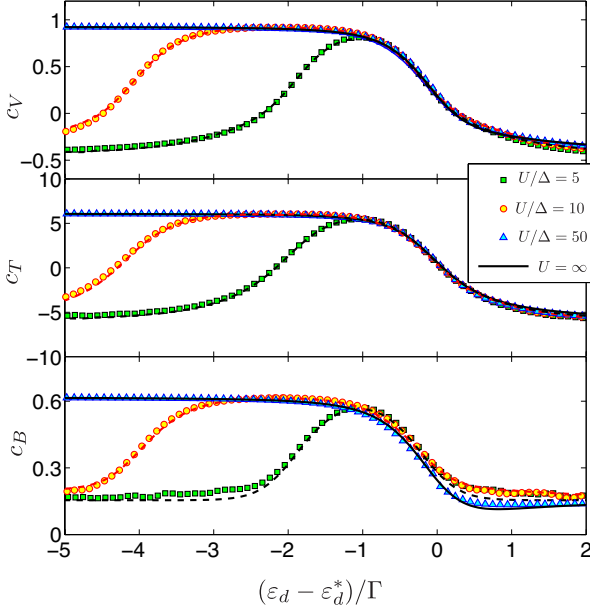


FIG. 8. (Color online) Approach to the mixed valence regime $U \rightarrow \infty$ for the transport Fermi-liquid coefficients c_V , c_T , and c_B computed using Bethe Ansatz (dashed lines) and the numerical renormalization group (symbols). The continuous black lines show the universal scaling curve in the $U \rightarrow \infty$ limit. By definition, the impurity occupancy is $n_d = 1/2$ for $\varepsilon_d = \varepsilon_d^*$.

determine the scale E^* in Eq. (6), expressed from (5) as

$$E^* = \frac{1}{4\chi_s + \chi_c}. \quad (50)$$

While measuring the gate voltage dependence of the charge on a quantum dot and thus χ_c is not very difficult, it is extremely hard to access the spin susceptibility χ_s in an ordinary quantum dot. Both χ_c and χ_s can, however, be measured in a spin-polarized capacitively coupled double quantum dot device [54], where charge degrees of freedom play the role of ordinary spin. In a large magnetic field, only spin-up electrons can stay on each quantum dot, and the number of electrons on the left and right dots, $\hat{n}_L = d_{L\uparrow}^\dagger d_{L\uparrow}$ and $\hat{n}_R = d_{R\uparrow}^\dagger d_{R\uparrow}$ play the same role as $\hat{n}_{d\uparrow} = d_{\uparrow}^\dagger d_{\uparrow}$ and $\hat{n}_{d\downarrow} = d_{\downarrow}^\dagger d_{\downarrow}$ in the Anderson model. In this case, both χ_c and χ_s can be determined from the side gate dependence of the occupations $\langle \hat{n}_R \rangle$ and $\langle \hat{n}_L \rangle$, monitored e.g. by point contact sensors.

While it is not very easy to measure the absolute values of the three transport coefficients, their *ratio* can be determined straightforwardly. The ratio c_V/c_B (presented in Fig. 9) also exhibit a non-trivial crossover between the Kondo and the empty-orbital regimes, characterized by universal functions in the $U \rightarrow \infty$ limit, and universal values in the Kondo and empty-orbital regimes, respectively.

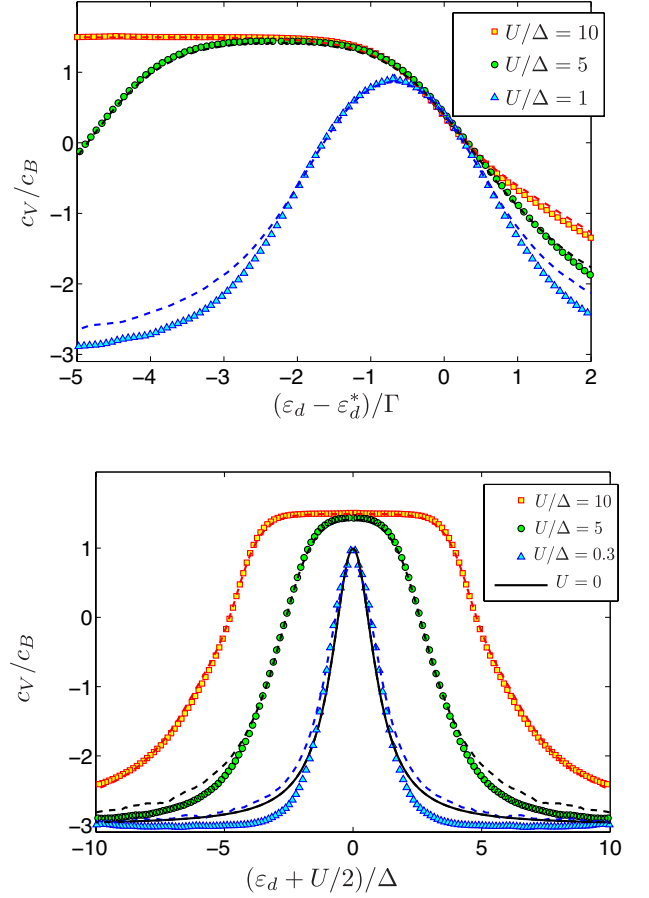


FIG. 9. (Color online) Upper panel: Plot of the ratios of the Fermi-liquid transport coefficients c_V/c_B as a function of $(\varepsilon_d - \varepsilon_d^*)/\Delta$ for different values of U/Δ , obtained using Bethe Ansatz (lines) and numerical renormalization group (symbols) calculations. Lower panel: The same ratios plotted as functions of $(\varepsilon_d + U/2)/\Delta$.

The quasiparticle Fermi-liquid theory presented here provides a simple and controlled framework to describe the leading behavior of the Anderson model at low temperatures, voltages, and magnetic fields. It should also be possible to obtain the results presented here with other methods such as renormalized perturbation theory (RPT) [20]. It is, however, not quite clear how the five parameters $\alpha_{1,2}$ and $\phi_{1,2}$ and the phase shift δ_0 , characterizing the generic quasiparticle Fermi-liquid theory would appear in RPT. Just as the underlying Anderson model, RPT has typically three parameters in its usual form, $\tilde{\varepsilon}_d$, \tilde{U} , and $\tilde{\Delta}$. It is not absolutely clear if these three parameters are sufficient to obtain the correct low temperature behavior, or if, similar to the quasiparticle Fermi-liquid theory, additional parameters need be introduced. The parameters $\alpha_{1,2}$ could be incorporated, e.g., via an energy dependent hybridization, $\Delta \rightarrow \Delta(\varepsilon)$, but the implementation of the irrelevant operator ϕ_2 does not seem to be entirely straightforward. Also, extracting ad-

ditional parameters of RPT directly from the finite size NRG spectrum [36] may run into technical difficulties.

Acknowledgement: We thank F. Bauer, J. Heyder, M. Kiselev and D. Schuricht for insightful comments and lively discussions. This work has been supported by the Hungarian research fund OTKA under grant Nos. K105149, by the UEFISCDI grant DYMESYS (ANR 2011-IS04-001-01, Contract No. PN-II-ID-JRP-2011-1), and the DFG via SFB-TR12, De730/4-3 and the NIM Cluster of Excellence.

Appendix A: Bethe Ansatz solution

1. Linear system

An exact solution to the ground state of the Anderson model can be derived using the Bethe Ansatz [2]. The description involves spin excitations with wavevector λ , corresponding to bound state singlet pairs, and unbound charge excitations with wavevector k . The densities of states $\sigma(\lambda)$ and $\rho(k)$ of these two types of excitations satisfy linear integral equations (to be written below) that can be solved either numerically or analytically in some parameter region with the help of the Wiener-Hopf method [2]. The system described by the spin and charge densities $\sigma(\lambda)$ and $\rho(k)$ corresponds to N electrons occupying either the dot single-level or the one-electron states of the conduction band. Since we consider a large number of electrons $N \gg 1$, the presence of the dot gives a subleading contribution to the densities

$$\sigma(\lambda) = \sigma_c(\lambda) + \frac{1}{L}\sigma_i(\lambda), \quad \rho(k) = \rho_c(k) + \frac{1}{L}\rho_i(k),$$

where the subscript c/i stands for conduction/impurity (dot), L is the system size increasing linearly with N .

$\sigma_c(\lambda)$ and $\rho_c(k)$ are the spin and charge densities in the absence of the dot. They describe, in fact, a free electron gas but in a complicated way. They are related to the external magnetic field B and the parameters of the Anderson model [39]

$$\frac{B}{2\pi} = \int_{-\infty}^{\Lambda} \rho_c(k) dk, \quad \frac{1}{\pi} \left(\varepsilon_d + \frac{U}{2} \right) = \int_{-\infty}^Q \sigma_c(\lambda) d\lambda,$$

where Λ and Q denote the chemical potentials of the unbound charge and spin excitations respectively. We have $Q = -\infty$ at the particle-hole symmetric point ($\varepsilon_d = -U/2$) and spin excitations are absent in the ground state. Similarly, unbound charges do not exist without external magnetic field and $\Lambda = -\infty$ in that case.

The impurity spin and charge densities $\sigma_i(\lambda)$ and $\rho_i(k)$ describe changes in the ground state when the coupling to the dot is included. They are related to the occupation

number n_d and the magnetization $m_d = (n_{d\uparrow} - n_{d\downarrow})/2$ of the dot through [39]

$$m_d = \frac{1}{2} \int_{-\infty}^{\Lambda} \rho_i(k) dk, \quad n_d = 1 - \int_{-\infty}^Q \sigma_i(\lambda) d\lambda, \quad (\text{A1})$$

and we recover the fact that $n_d = 1$ at the particle-hole symmetric point, and $m_d = 0$ when no magnetic field is applied.

The densities $\sigma_c(\lambda)$, $\rho_c(k)$, $\sigma_i(\lambda)$ and $\rho_i(k)$, characterizing the ground state, are solution of the coupled linear integral equations ($a = c/i$)

$$\begin{aligned} \rho_a(k) + g'(k) \int_{-\infty}^{\Lambda} dk' R[g(k) - g(k')] \rho_a(k') \\ + g'(k) \int_{-\infty}^Q d\lambda s[g(k) - \lambda] \sigma_a(\lambda) = \mathcal{S}_{a,1}(k), \end{aligned} \quad (\text{A2a})$$

$$\begin{aligned} \sigma_a(\lambda) - \int_{-\infty}^Q d\lambda' R(\lambda - \lambda') \sigma_a(\lambda') \\ + \int_{-\infty}^{\Lambda} dk s[\lambda - g(k)] \rho_a(k) = \mathcal{S}_{a,2}(\lambda). \end{aligned} \quad (\text{A2b})$$

The conduction and impurity equations differ only by the source term in the right-hand-side

$$\mathcal{S}_{c,1}(k) = \frac{1}{2\pi} \left[1 + g'(k) \int_{-\infty}^{+\infty} dk' R[g(k) - g(k')] \right],$$

$$\mathcal{S}_{c,2}(\lambda) = \frac{1}{2\pi} \int_{-\infty}^{+\infty} dk s[\lambda - g(k)],$$

$$\mathcal{S}_{i,1}(k) = \Delta(k) + g'(k) \int_{-\infty}^{+\infty} dk' R[g(k) - g(k')] \Delta(k'),$$

$$\mathcal{S}_{i,2}(\lambda) = \int_{-\infty}^{+\infty} dk s[\lambda - g(k)] \Delta(k),$$

with the definitions

$$R(x) = \frac{1}{2\pi} \int_{-\infty}^{+\infty} d\omega \frac{e^{-i\omega x}}{1 + e^{|\omega|}}, \quad (\text{A3a})$$

$$s(x) = \frac{1}{2 \cosh(\pi x)}, \quad (\text{A3b})$$

$$g(k) = \frac{1}{2U\Delta} (k - \varepsilon_d - U/2)^2, \quad (\text{A3c})$$

$$\Delta(k) = \frac{1}{\pi} \frac{\Delta}{(k - \varepsilon_d)^2 + \Delta^2}. \quad (\text{A3d})$$

2. Wiener-Hopf solution

A complete analytical solution to the coupled equations (A2) does not exist in the general case, for which they can be solved numerically. Nevertheless, analytical

progress is possible close to the particle-hole symmetric point, or for a weak magnetic field, in which cases the two equations decouple.

At zero magnetic field $\Lambda = -\infty$ and the second integral equations simplify to

$$\sigma_a(\lambda) - \int_{-\infty}^Q d\lambda' R(\lambda - \lambda') \sigma_a(\lambda') = \mathcal{S}_{a,2}(\lambda). \quad (\text{A4})$$

These two equations are solvable by the Wiener-Hopf technique. Details on this calculation can be found in the review [2]. The result is a parametric expression of n_d as a function of ε_d via the chemical potential Q , namely

$$\begin{aligned} \varepsilon_d = & -\frac{U}{2} + \sqrt{2U\Delta Q} \theta(Q) - \frac{\sqrt{U\Delta}}{2\pi^{3/2}} \text{Re} \left[\frac{1}{\sqrt{i}} \int_0^{+\infty} d\omega \right. \\ & \times \frac{e^{-2iQ\pi\omega}}{\omega^{3/2}} \left\{ e^{-\pi\omega} \left(\frac{e}{i\omega} \right)^{i\omega} \Gamma\left(\frac{1}{2} + i\omega\right) - \sqrt{\pi} \right\} \Big], \end{aligned} \quad (\text{A5})$$

or, alternatively,

$$\begin{aligned} \varepsilon_d = & -\frac{U}{2} + 2\sqrt{\frac{U\Delta}{2\pi}} \sum_{n=0}^{+\infty} \frac{(-1)^n}{n!(1+2n)^{3/2}} \left(\frac{n+1/2}{e} \right)^{n+1/2} \\ & + \frac{\sqrt{U\Delta}}{2\pi^{3/2}} \text{Re} \left[\frac{1}{\sqrt{i}} \int_0^{+\infty} d\omega \frac{1 - e^{-2iQ\pi\omega}}{\omega^{3/2}} \right. \\ & \times e^{-\pi\omega} \left(\frac{e}{i\omega} \right)^{i\omega} \Gamma\left(\frac{1}{2} + i\omega\right) \Big], \end{aligned} \quad (\text{A6})$$

both valid for all Q . $\Gamma(z)$ denotes the gamma function. An alternative summation can be found in Ref. [2] for $Q < 0$ but it does not yield a sizeable numerical speed-up. The second expression is

$$\begin{aligned} n_d = & \frac{1}{2} - \frac{1}{\pi^{3/2}} \text{Re} \left[\int_0^{+\infty} i d\omega \frac{e^{-2iQ\pi\omega}}{\omega} e^{-\pi\omega} \left(\frac{e}{i\omega} \right)^{i\omega} \right. \\ & \times \Gamma\left(\frac{1}{2} + i\omega\right) \int_{-\infty}^{+\infty} \frac{dx}{\pi} \frac{e^{i\pi\omega x^2 \Delta/U}}{1 + (x + U/2\Delta)^2} \Big]. \end{aligned} \quad (\text{A7})$$

Eqs. (A5) and (A7) can be used to compute n_d and therefore δ_0 . The charge susceptibility χ_c is obtained from the derivatives of these two expressions with respect to Q , and

$$\chi_c = -\frac{\partial n_d / \partial Q}{\partial \varepsilon_d / \partial Q}.$$

In order to compute the spin susceptibility, we need to add a small magnetic field. The two equations (A2) are then weakly coupled and can be solved perturbatively at low magnetic field [2]. The result for the spin susceptibility at zero magnetic field is finally given by

$$\chi_s = \frac{e^{\pi Q} \bar{\sigma}_i + e^{\pi/I} + \int_x \frac{1}{\pi} \frac{e^{-\pi x^2 \Delta/2U}}{1 + (ix + U/2\Delta)^2}}{2\sqrt{2U\Delta} + 4\pi\sqrt{U\Delta} e^{\pi Q} \bar{\sigma}_c}, \quad (\text{A8})$$

where $1/I = U/8\Delta - \Delta/2U$, with

$$\begin{aligned} \bar{\sigma}_c = & -\frac{1}{2\pi^2 \sqrt{2e}} \text{Re} \left[\int_0^{+\infty} d\omega \frac{e^{-2iQ\pi\omega}}{\omega + i/2} \right. \\ & \times \frac{e^{-\pi\omega}}{\sqrt{i\omega}} \left(\frac{e}{i\omega} \right)^{i\omega} \Gamma\left(\frac{1}{2} + i\omega\right) \Big], \end{aligned} \quad (\text{A9})$$

and

$$\begin{aligned} \bar{\sigma}_i = & \frac{1}{\pi\sqrt{2e}} \text{Re} \left[\int_0^{+\infty} i d\omega \frac{e^{-2iQ\pi\omega}}{\omega + i/2} e^{-\pi\omega} \left(\frac{e}{i\omega} \right)^{i\omega} \right. \\ & \times \Gamma\left(\frac{1}{2} + i\omega\right) \int_{-\infty}^{+\infty} \frac{dx}{\pi} \frac{e^{i\pi\omega x^2 \Delta/U}}{1 + (x + U/2\Delta)^2} \Big]. \end{aligned} \quad (\text{A10})$$

3. Mixed-valence regime

The Bethe Ansatz solutions derived in Sec. A2 for n_d and χ_s simplify substantially in the mixed-valence limit where $U \rightarrow \infty$ with fixed ε_d and Δ . In this limit, the chemical potential Q becomes very large. It can be absorbed into the definition of a renormalized single-particle energy

$$2\Delta Q - \frac{U}{4} = \varepsilon_{dR} = \varepsilon_d + \frac{\Delta}{\pi} \ln \left(\frac{\pi e U}{4\Delta} \right). \quad (\text{A11})$$

This result is obtained because we took the limit of large U after taking the limit of an infinite cutoff for the Anderson model. If the opposite is done, the same theory applies by with the model high-energy cutoff (bandwidth) replacing U in Eq. (A11). All observables are now universal functions of ε_{dR} and Δ , namely the dot occupancy is given by

$$\begin{aligned} n_d = & \frac{1}{2} - \frac{1}{\pi^{3/2}} \int_0^{+\infty} d\omega e^{-2\pi\omega} \text{Re} \left[i \frac{e^{-i\pi\omega \varepsilon_{dR}/\Delta}}{\omega} \right. \\ & \times \Gamma\left(\frac{1}{2} + i\omega\right) \left(\frac{e}{i\omega} \right)^{i\omega} \Big]. \end{aligned} \quad (\text{A12})$$

This expression is suitable for fast numerical calculation thanks to its exponential convergence. It is also easy to differentiate, the charge susceptibility then takes the form

$$\begin{aligned} \chi_c = & \frac{1}{\sqrt{\pi}\Delta} \int_0^{+\infty} d\omega e^{-2\pi\omega} \text{Re} \left[e^{-i\pi\omega \varepsilon_{dR}/\Delta} \right. \\ & \times \Gamma\left(\frac{1}{2} + i\omega\right) \left(\frac{e}{i\omega} \right)^{i\omega} \Big]. \end{aligned} \quad (\text{A13})$$

The spin susceptibility also simplifies to

$$\begin{aligned} \chi_s = & \frac{\sqrt{2\pi e}}{8\Delta} e^{-\pi \varepsilon_{dR}/(2\Delta)} + \frac{1}{8\sqrt{\pi}\Delta} \int_0^{+\infty} d\omega \\ & e^{-2\pi\omega} \text{Re} \left[i \frac{e^{-i\pi\omega \varepsilon_{dR}/\Delta}}{\omega + i/2} \Gamma\left(\frac{1}{2} + i\omega\right) \left(\frac{e}{i\omega} \right)^{i\omega} \right]. \end{aligned} \quad (\text{A14})$$

Appendix B: Empty-orbital regime

In this Appendix, we examine the empty-orbital regime $\varepsilon_d \gg \Delta$ using standard perturbation theory (Rayleigh-Schrödinger). The unperturbed state is for $t = 0$ (or $\Delta = 0$), it corresponds to an empty impurity level with a filled zero-temperature Fermi sea. Perturbation theory is carried out with respect to the tunneling of electrons between the impurity and the conduction sea. The unnormalized wavefunction of the ground state $|\psi\rangle$ is computed to third order in t . The impurity occupancy is then given by

$$n_d = \frac{\langle \psi | \hat{n}_d | \psi \rangle}{\langle \psi | \psi \rangle}. \quad (\text{B1})$$

The results are too cumbersome to be written in full details here. However, they simplify in the limit $U \gg \varepsilon_d$ and $U \ll \varepsilon_d$.

In the former case $U \gg \varepsilon_d$, we obtain the asymptotic expressions

$$\chi_c = \frac{2\Delta}{\pi\varepsilon_d^2} \left[1 + \frac{2\Delta}{\pi\varepsilon_d} \left\{ -\frac{3}{2} + \ln\left(\frac{\varepsilon_d}{U}\right) \right\} \right], \quad (\text{B2})$$

for the charge susceptibility and

$$\chi_s = \frac{\Delta}{2\pi\varepsilon_d^2} \left[1 + \frac{2\Delta}{\pi\varepsilon_d} \left\{ \frac{1}{2} + \ln\left(\frac{\varepsilon_d}{U}\right) \right\} \right], \quad (\text{B3})$$

for the spin susceptibility, in agreement with Haldane [55]. Eq. (B2) and Eq. (B3) can also be derived from the mixed-valence results Eq. (A13) and Eq. (A14) in the limit $\varepsilon_{dR} \gg \Delta$.

In the latter case $U \ll \varepsilon_d$, the results are

$$n_d = \frac{2\Delta}{\pi\varepsilon_d} \left[1 - \frac{\Delta U}{\pi\varepsilon_d^2} \right], \quad (\text{B4})$$

and

$$\chi_s = \frac{\Delta}{2\pi\varepsilon_d^2} \left[1 - \frac{\Delta U}{\pi\varepsilon_d^2} \right]. \quad (\text{B5})$$

The Fermi-liquid parameters can be deduced from these expressions using Eqs. (5). To leading order in Δ/ε_d the parameters α_1 and α_2 that describe elastic scattering do not depend on the ratio of U/ε_d . They are given by

$$\begin{aligned} \alpha_1 &= \pi \left(\chi_s + \frac{\chi_c}{4} \right) \simeq \frac{\Delta}{\varepsilon_d^2}, \\ \alpha_2 &= -\pi \left(\frac{3}{4} \chi'_s + \frac{\chi'_c}{16} \right) \simeq \frac{\Delta}{\varepsilon_d^3}, \end{aligned} \quad (\text{B6})$$

corresponding to the phase shift expansion of a non-interacting resonant level model $\delta(\varepsilon) = \text{atan}[\Delta/(\varepsilon_d - \varepsilon)]$. The parameters ϕ_1 and ϕ_2 that describe interaction processes depend on U/ε_d . They are given by

$$\phi_1 = \pi \left(\chi_s - \frac{\chi_c}{4} \right) \simeq \frac{2\Delta^2}{\pi\varepsilon_d^3} \quad \phi_2 = -\phi'_1 = \frac{6\Delta^2}{\pi\varepsilon_d^4}, \quad (\text{B7})$$

for $U \gg \varepsilon_d$ and

$$\phi_1 = \frac{\Delta^2 U}{\pi\varepsilon_d^4} \quad \phi_2 = -\phi'_1 = \frac{4\Delta^2 U}{\pi\varepsilon_d^5}, \quad (\text{B8})$$

for $U \ll \varepsilon_d$. The corresponding FL transport coefficients are given by Eq. (8).

-
- [1] G. Grüner and A. Zawadowski, Rep. Prog. Phys. **37**, 1497 (1974)
 - [2] A. Tsvelick and P. Wiegmann, Adv. Phys. **32**, 453 (1983)
 - [3] A. C. Hewson, *The Kondo Problem to Heavy Fermions* (Cambridge University Press, Cambridge, 1993)
 - [4] L. Glazman and M. Pustilnik, in *New Directions in Mesoscopic Physics (Towards Nanoscience)*, edited by R. Fazio, V. Gantmakher, and Y. Imry (Kluwer, Dordrecht, 2003) J. Phys.: Condens. Matter **16**, R513 (2004)
 - [5] A. M. Chang and J. C. Chen, Rep. Prog. Phys. **72**, 096501 (2009)
 - [6] A. Georges, G. Kotliar, W. Krauth, and M. J. Rozenberg, Rev. Mod. Phys. **68**, 13 (1996)
 - [7] D. L. Cox and A. Zawadowski, Adv. Phys. **47**, 599 (1998)
 - [8] P. Coleman, in *Handbook of Magnetism and Advanced Magnetic Materials Vol. 1*, edited by H. Kronmüller and S. Parkin (Wiley, 2007) pp. 95–148
 - [9] In fact, the Kondo limit can be formally extended to the region $\varepsilon_d/U \in [-1, 0]$ when $U/\Delta \rightarrow \infty$. In this limit, the potential scattering term, which breaks particle-hole symmetry, vanishes [3].
 - [10] J. R. Schrieffer and P. A. Wolff, Phys. Rev. **149**, 491 (1966)
 - [11] J. Kondo, Prog. Theor. Phys. **32**, 37 (1964)
 - [12] K. G. Wilson, Rev. Mod. Phys. **47**, 773 (1975)
 - [13] P. Nozières, J. Low Temp. Phys. **17**, 31 (1974) in *Proceedings of the 14th International Conference on Low Temperature Physics*, Vol. 5, edited by M. Krasius and M. Vuorio (North Holland, Amsterdam, 1974) pp. 339–374 J. Physique **39**, 1117 (1978)
 - [14] K. Yosida and K. Yamada, Prog. Theor. Phys. **46**, 244 (1970) K. Yamada, **53**, 970 (1975) K. Yosida and K. Yamada, Prog. Theor. Phys. **53**, 1286 (1975) K. Yamada, Prog. Theor. Phys. **54**, 316 (1975)
 - [15] A. Yoshimori, Prog. Theor. Phys. **55**, 67 (1976)
 - [16] L. Mihály and A. Zawadowski, J. Phys. (Paris) Lett. **39**, 483 (1978)
 - [17] C. B. M. Hørig, C. Mora, and D. Schuricht, Phys. Rev.

- B **89**, 165411 (2014)
- [18] M. Hanl, A. Weichselbaum, J. von Delft, and M. Kiselev, *Phys. Rev. B* **89**, 195131 (2014)
- [19] A. Oguri, *Phys. Rev. B* **64**, 153305 (Sep 2001)
- [20] A. C. Hewson, *Phys. Rev. Lett.* **70**, 4007 (1993) *J. Phys.: Condens. Matter* **5**, 6277 (1993) *Adv. Phys.* **43**, 543 (1994)
- [21] A. C. Hewson, *J. Phys.: Condens. Matter* **13**, 10011 (2001) A. C. Hewson, A. Oguri, and D. Meyer, *Eur. Phys. J. B* **40**, 177 (2004) A. C. Hewson, *J. Phys.: Condens. Matter* **18**, 1815 (2006) A. C. Hewson, J. Bauer, and W. Koller, *Phys. Rev. B* **73**, 045117 (2006) J. Bauer and A. C. Hewson, **76**, 035119 (2007) K. Edwards and A. C. Hewson, *J. Phys.: Condens. Matter* **23**, 045601 (2011) K. Edwards, A. C. Hewson, and V. Pandis, *Phys. Rev. B* **87**, 165128 (2013)
- [22] S. Streib, A. Isidori, and P. Kopietz, *Phys. Rev. B* **87**, 201107 (May 2013)
- [23] T. Fujii, *J. Phys. Soc. Jpn.* **79** (2010)
- [24] R. Sakano, T. Fujii, and A. Oguri, *Phys. Rev. B* **83**, 075440 (2011)
- [25] R. Sakano, A. Oguri, T. Kato, and S. Tarucha, *Phys. Rev. B* **83**, 241301 (2011)
- [26] L. Glazman and M. Pustilnik, in *Nanophysics: Coherence and Transport*, edited by H. *et al.*. Bouchiat (Elsevier, Amsterdam, 2005) pp. 427–478, cond-mat/0501007
- [27] E. Sela, Y. Oreg, F. von Oppen, and J. Koch, *Phys. Rev. Lett.* **97**, 086601 (2006)
- [28] A. Golub, *Phys. Rev. B* **73**, 233310 (2006)
- [29] A. O. Gogolin and A. Komnik, *Phys. Rev. Lett.* **97**, 016602 (2006)
- [30] C. Mora, X. Leyronas, and N. Regnault, *Phys. Rev. Lett.* **100**, 036604 (2008)
- [31] C. Mora, *Phys. Rev. B* **80**, 125304 (2009)
- [32] C. Mora, P. Vitushinsky, X. Leyronas, A. A. Clerk, and K. Le Hur, *Phys. Rev. B* **80**, 155322 (2009)
- [33] P. Vitushinsky, A. A. Clerk, and K. Le Hur, *Phys. Rev. Lett.* **100**, 036603 (2008)
- [34] E. Sela and J. Malecki, *Phys. Rev. B* **80**, 233103 (Dec 2009)
- [35] F. D. M. Haldane, *Phys. Rev. Lett.* **40**, 416 (1978)
- [36] H. R. Krishna-murthy, J. W. Wilkins, and K. G. Wilson, *Phys. Rev. B* **21**, 1003 (1980) **21**, 1044 (1980)
- [37] E. Muñoz, C. J. Bolech, and S. Kirchner, *Phys. Rev. Lett.* **110**, 016601 (2013)
- [38] L. Merker, S. Kirchner, E. Muñoz, and T. A. Costi, *Phys. Rev. B* **87**, 165132 (2013)
- [39] N. Kawakami and A. Okiji, *J. Phys. Soc. Jpn.* **51**, 2043 (1982)
- [40] A. Tselick and P. Wiegmann, *J. Phys. C* **16**, 2321 (1983)
- [41] A. V. Kretinin, H. Shtrikman, D. Goldhaber-Gordon, M. Hanl, A. Weichselbaum, J. von Delft, T. Costi, and D. Mahalu, *Phys. Rev. B* **84**, 245316 (2011)
- [42] F. Lesage and H. Saleur, *Phys. Rev. Lett.* **82**, 4540 (1999) *Nucl. Phys. B* **546**, 585 (1999)
- [43] L. Landau, *Soviet Phys. JETP* **3**, 920 (1957) **5**, 101 (1957)
- [44] P. Nozieres, *Theory of interacting Fermi systems* (Addison-Wesley, 1964)
- [45] This implies in particular that the arbitrary energy ε_0 must be chosen near the zero-temperature chemical potential μ_0 , $|\varepsilon_0 - \mu_0| \ll E^*$.
- [46] C. Mora, X. Leyronas, and N. Regnault, *Phys. Rev. Lett.* **102**, 139902(E) (2009)
- [47] Further terms arise, proportional to α'_2 or ϕ'_2 times term quadratic in ε , but we ignore these, since they are of similar order as ones that would have arisen had Eq. (14) included terms cubic in ε , which we neglected.
- [48] J. Friedel, *Can. J. Phys.* **34**, 1190 (1956)
- [49] In Eq. (3), normal ordering is w.r.t. to a reference state with chemical potential $\varepsilon_0 = 0$. Its form for $\varepsilon_0 \neq 0$ is obtained by replacing $\varepsilon_i \rightarrow \varepsilon_i - \varepsilon_0$ in the coefficients of α_1 , α_2 and ϕ_2 , and by normal ordering w.r.t. to ε_0 .
- [50] Y. M. Blanter and M. Büttiker, *Phys. Rep.* **366**, 1 (2000)
- [51] A. Kamenev and A. Levchenko, *Adv. Phys.* **58**, 197 (2009)
- [52] J. Rincón, A. A. Aligia, and K. Hallberg, *Phys. Rev. B* **79**, 121301 (2009) *Phys. Rev. B (E)* **80**, 079902 (2009) **81**, 039901 (2010)
- [53] We used the open-access Budapest Flexible DM-NRG code, <http://www.phy.bme.hu/~dmnrg/>; O. Legeza, C. P. Moca, A. I. Tóth, I. Weymann, G. Zaránd, arXiv:0809.3143 (2008) (unpublished)
- [54] S. Amasha, A. J. Keller, I. G. Rau, A. Carmi, J. A. Katiné, H. Shtrikman, Y. Oreg, and D. Goldhaber-Gordon, *Phys. Rev. Lett.* **110**, 046604 (2013)
- [55] F. D. M. Haldane, *J. Phys. C: Solid State Phys.* **11**, 5015 (1978)